



HAL
open science

Mode computation of immersed multilayer plates by solving an eigenvalue problem

Eric Ducasse, Marc Deschamps

► **To cite this version:**

Eric Ducasse, Marc Deschamps. Mode computation of immersed multilayer plates by solving an eigenvalue problem. *Wave Motion*, 2022, 112, pp.102962. 10.1016/j.wavemoti.2022.102962 . hal-03758722

HAL Id: hal-03758722

<https://hal.science/hal-03758722>

Submitted on 23 Aug 2022

HAL is a multi-disciplinary open access archive for the deposit and dissemination of scientific research documents, whether they are published or not. The documents may come from teaching and research institutions in France or abroad, or from public or private research centers.

L'archive ouverte pluridisciplinaire **HAL**, est destinée au dépôt et à la diffusion de documents scientifiques de niveau recherche, publiés ou non, émanant des établissements d'enseignement et de recherche français ou étrangers, des laboratoires publics ou privés.

Mode computation of immersed multilayer plates by solving an eigenvalue problem

Eric Ducasse^{1,3,4} eric.ducasse@u-bordeaux.fr

Marc Deschamps^{1,2} marc.deschamps@u-bordeaux.fr

¹ Univ. Bordeaux, *I₂M-APy*, UMR 5295, F-33400 Talence, France.

² CNRS, *I₂M-APy*, UMR 5295, F-33400 Talence, France.

³ Arts et Metiers ParisTech, *I₂M-APy*, UMR 5295, F-33400 Talence, France.

⁴ Corresponding author. Tel. +33(0)540003138. Fax +33(0)540006964.

Abstract

The aim of this paper is to compute modes of immersed multilayer plates by writing and solving an eigenvalue problem. The method can be applied to any kind of material with layers, *i.e.*, fluid, anisotropic and viscoelastic. The two external interfaces of the plate can be described as either vacuum/vacuum, fluid/vacuum, or fluid/fluid with a single fluid or fluid/fluid with two different fluids. The method is based on the discretization of the plate by using a finite differences scheme in its vertical direction. One global state vector is associated with inner discretized positions of each layer, and two local state vectors characterize the physical state at its bounds. Interfacial state vectors are introduced in certain situations at external and internal plate interfaces. With these state vectors and after pertinent algebraic manipulations, an eigenvalue system is built. Its solutions are searched by fixing the slowness, wavevector or frequency of guided waves. These three parameterizations correspond to three different physical models. For each case, discussions of dispersion curves and attenuation curves are given for guided modes in a plate loaded by fluids at one or two sides. This numerical tool is shown to provide convenience and accuracy.

keyword

Ultrasonic Waveguide; Immersed Multilayer Plate; Mode Computation; Formulation of an Eigenvalue Problem; Exact Boundary Condition; Dispersion and Attenuation Curves; Global, Local and Interfacial State Vectors.

highlights

- The computation of modes is accomplished by writing and solving an eigenvalue problem.
- Guided modes are found for a given slowness, wavevector or frequency.
- Convenient global, local and interfacial state vectors are necessary to build an eigenvalue system.
- A plate can possibly be loaded by two fluids with different sound speeds.

1 Introduction

The subject of this paper is to provide a method that efficiently computes modes in multilayer plates that are fluid-loaded on one or both sides by building an eigenvalue problem. In a one- or two-dimensional waveguide, a mode is characterized by its wavevector $\mathbf{k} = \omega \mathbf{s}$ belonging to the axis/plane of the waveguide, its slowness vector \mathbf{s} and its angular frequency ω . Without any treatment, a linear system $\mathcal{L}(\mathbf{k}, \omega) \mathbf{a} = \mathbf{0}$ can be written. The global matrix $\mathcal{L}(\mathbf{k}, \omega)$ [19] characterizes the waveguide, while components of the vector \mathbf{a} that are not all zeros are the amplitudes of the partial waves [26] contributing to the mode shape. The existence of a nonzero solution \mathbf{a} is conditioned by the satisfaction of the so-called “dispersion equation” $\det[\mathcal{L}(\mathbf{k}, \omega)] = 0$. This strongly nonlinear equation can be directly solved by standard root-finding methods, for example Newton-like iterative methods [19, 26]. The solutions of the dispersion equation are found one by one, with frequent problems of convergence or ill-conditioning.

Alternatively, to avoid such numerical problems, an eigenvalue problem, which is easily solved with all solutions acquired by a single computation, can be formulated by spatial discretization of the waveguide cross-section. Specifically for nonradiating waveguides, various methods have been developed over the last decades to make this discretization. As examples of such methods, let us cite the following: the thin-layer method (TLM) [14, 17], the semi-analytical finite element (SAFE) approach [6], the scaled boundary finite element method (SBFEM) [7], the high-order finite difference scheme [3], spectral collocation [12, 18], the complex-length finite element method (CFEM) [1], or decomposition on basis functions [24].

For immersed or embedded one-dimensional waveguides, such as rods and pipes, two main approaches have been used to obtain an eigenvalue problem. First, approximate radiation boundary conditions can be formulated as in [13] for the fluid-loaded case and in [9, 10] for the solid-loaded case, namely, the dashpot boundary condition. Second, numerical techniques for modeling the external infinite medium can be performed, such as “absorbing regions” for fluids [4] and solids [2], the 2.5D boundary element method for fluids [21] and solids [20], and perfectly matched layers (PML) for fluids [31] and solids [23]. Alternatively, iterative computation by solving successive eigenvalue problems has also been used [8]. For a more complete bibliography, see, *e.g.*, [8, 11, 21, 1, 18].

Even if similar methods can be directly employed for multilayer plates, *e.g.*, [8, 30, 5], some specific and useful approaches have been introduced. In that respect, for a solid half-space in seismology, the CFEM is coupled with the method of perfectly matched discrete layers (PMDL) in [1]. More important for our study are recent works of great interest on plates for an external fluid either on one side or both sides of the plate. In this way, exact formulations have been developed to achieve a “polynomial eigenvalue problem” either directly by “*using the symmetry of Lamb wave modes under the conditions that leaky media are nonviscous fluids with the same sound velocities*” with SAFE [11], or by a change of variable in a spectral collocation scheme [18].

The present paper is in line with the results of Hayashi and Inoue [11] and of Kiefer *et al.* [18], which to our knowledge are the only publications that have successfully posed an eigenvalue problem with exact boundary conditions for an immersed plate. Even though the essence of these two methods and of ours may be the same, the obtained final systems are significantly different since their specific state vectors have nothing to do with each other. In addition, the polynomial eigenvalue formulations in [11] and [18] are not involved here. This leads to a numerically solvable problem of smaller dimension. Moreover, the articles [11] and [18] are limited to the case where the plate is loaded by two external fluids with the same sound speed. Another advance of the present work is the use of a high-order finite difference scheme chosen for the simplicity of its implementation. It also has other advantages such as very good accuracy with relatively few discretization points and the fact that it does not require using any external calculation code.

The present paper addresses the case of a fluid-loaded multilayer plate where the two external fluids can have different sound speeds. The global eigenvalue problem is built from a primary linear problem involving so-called “global state vectors” and “local state vectors”. A single global state vector entirely describes the inner physical state of the plate and depends on the numerical scheme used to discretize the plate thickness. At most two local state vectors, introduced if necessary, represent the physical state of the plate at its external interfaces and are involved in the boundary conditions. These boundary conditions are the classical zero normal stress condition for vacuum, zero normal displacement for a rigid wall or the exact radiation boundary condition for an external fluid.

The dimension of the final eigenvalue problem is approximately twice the initial problem dimension if either a fluid is loading one side only or if the two loading fluids have the same sound speed. This final dimension is approximately four times the initial problem dimension if the two loading fluids have different sound speeds. Thus, each frequency–wavenumber pair found numerically corresponds to a nonzero solution of wave equations such that the acoustic wave in each external fluid is a plane wave with a single wavevector.

Consequently, the present technique is convenient not only to compute “guided modes”, where the plate does radiate into one or two external fluids or does not for SH waves but also to deal with “crossing modes”, for which an incident acoustic wave comes from one side of the plate and is transmitted through the plate to its other side without any reflection. This point should be kept in mind for interpreting the results, even if it will not be emphasized in this paper.

For lossless waveguides, the propagative modes have real-valued wavenumbers and, consequently, real-valued slownesses, while evanescent modes have complex wavenumbers and amplitudes rapidly decreasing in space. For radiating waveguides, a leaky mode can be characterized by its frequency, its wavenumber and its slowness. Only one of these three parameters can be real-valued while the other two are complex-valued with nonzero imaginary parts due to the leakage. Concerning these three parameters, different cases must be analyzed separately: (i) In almost all of the papers cited above, as in most literature on the subject regardless of the technique used, the axial wavenumbers of the modes are computed for a given real-valued frequency. This is what is called the *fixed-frequency problem*. (ii) It has been shown that field computation can be done by a modal approach in the time domain by computing eigenfrequencies for given real wavenumbers [17, 3]. As a result, the complete modal basis contains only the propagative modes. Curiously, to our knowledge, these techniques are used relatively infrequently. In the same idea, efficient codes using Laplace and Fourier integral transforms exist for simulating the wave propagation in immersed/embedded waveguides of canonical forms, *e.g.*, multilayer plates [15, 22] and multilayer axisymmetric pipes [16]. For these two ways to calculate fields in waveguides, *i.e.*, modal expansion in time and integral transforms, the wavenumber is fixed and assumed to be real. This is the *fixed-wavenumber problem*. (iii) To fully explain phenomena observed in experimental or numerical studies, due to plate resonances, it is of great interest to fix a real-valued slowness [27]. This is the so-called *fixed-slowness problem*.

These three *problems*, which correspond to three different types of modes, are addressed below and illustrated by basic examples. It is shown that for high-order finite difference schemes, detailed in the appendices, the first two *problems* can be treated by the general technique described in this paper, while the last case, *i.e.*, the *fixed-slowness problem*, does not need particular treatment for immersed/embedded plates. In the latter case, in contrast, possible ill-posed situations and singularities can occur and must be taken into account.

2 Definitions and basic equations

Let us consider a multilayered medium made of a plate system consisting of m number of perfect flat layers of normal \mathbf{z} corresponding to the vertical direction. The plate is assumed to be infinite in the horizontal xy -plane and any two layers in contact are stacked together in this plane. Each layer is made either of an anisotropic solid or a fluid, with a given thickness $h_\beta = z_\beta - z_{\beta-1}$, as illustrated in Fig. 1. The total thickness is expressed by ℓ . Above and below this plate system are semi-infinite half-spaces of fluid or vacuum. Without loss of generality, we consider that each mode is characterized by its displacement field:

$$\underline{\mathbf{u}}(x, y, z, t) = \text{Re}\{\mathbf{u}(z) \exp[\mathbf{i}(\omega t - kx - \nu y)]\}$$

at any time t and observation point $\mathbf{m} = (x, y, z)$. Satisfying the Snell-Descartes law at each interface, the wavenumbers k and ν in the x - and y -directions, respectively, are identical for all partial waves propagating in any layer or half-space. The complex function \mathbf{u} results in interferences of these partial waves within the plate. Without loss of generality, the wavenumber $k = k_r + \mathbf{i}k_i$ can be complex-valued, while the wavenumber ν is considered a fixed real-valued parameter. The complex angular frequency $\omega = \omega_r + \mathbf{i}\omega_i$ satisfies $\omega_r \geq 0$, and the amplitude is either constant or decreasing in time, *i.e.*, $\omega_i \geq 0$, if the plate can radiate outwardly. In contrast, the amplitude will be increasing, *i.e.*, $\omega_i < 0$, if the plate receives energy from the outside.

Consequently, each mode is characterized here by its angular frequency ω , its wavenumber k in the x -direction and its shape $\mathbf{u}(z)$. Hereafter, for convenience, any shape $f(z)$ of a field $\underline{f}(x, y, z, t)$ will be directly called by the field name, *e.g.*, $\mathbf{u}(z)$ will be the displacement vector. Furthermore, in all the equations below, the symbols prime and double prime indicate, respectively, the first and second derivatives with respect to the vertical z -direction. The wavenumber ν in the y -direction is often zero but it can be useful to consider it as a fixed real-valued parameter to stay as general as possible.

The multilayer plate can contain solid and fluid layers, while each of its external bounds is in contact either with vacuum¹ or a fluid. Let us now summarize the basic equations of wave propagation in these media.

2.1 Solid media

First, solid layers are considered by assuming a general viscoelastic model. Due to possible stratification, the mass density $\rho(z)$ depends on the vertical position z . Newton's second law yields the following system of equations:

$$-\rho(z)\omega^2 \mathbf{u}(z) = -\mathfrak{i} k \boldsymbol{\sigma}_x(z) - \mathfrak{i} \nu \boldsymbol{\sigma}_y(z) + \boldsymbol{\sigma}'_z(z), \quad (1)$$

where the vector $\boldsymbol{\sigma}_\alpha(z)$ stands for the stress vector in the α -direction.

The generalized Hooke's law is expressed by:

$$\begin{aligned} \boldsymbol{\sigma}_\alpha(z) = & -\mathfrak{i} k [\mathcal{C}_{\alpha x}(z) + \mathfrak{i} \omega \mathcal{H}_{\alpha x}(z)] \mathbf{u}(z) \\ & -\mathfrak{i} \nu [\mathcal{C}_{\alpha y}(z) + \mathfrak{i} \omega \mathcal{H}_{\alpha y}(z)] \mathbf{u}(z) \\ & + [\mathcal{C}_{\alpha z}(z) + \mathfrak{i} \omega \mathcal{H}_{\alpha z}(z)] \mathbf{u}'(z), \quad \alpha = x, y, z, \end{aligned} \quad (2)$$

which models a viscoelastic behavior by introducing complex elastic tensors $\mathcal{C}(z)$ and $\mathcal{H}(z)$ which can depend on the vertical position z . In addition, 3-by-3 submatrices of these tensors are involved in Eq. (2) and satisfy $\mathcal{M}_{\alpha\beta}(z) = [m_{\alpha ij\beta}(z)]_{1 \leq i \leq 3, 1 \leq j \leq 3}$, $\mathcal{M} = \mathcal{C}, \mathcal{H}$. With the exception of the symmetry conditions, no specific assumptions are imposed on these coefficients. Therefore, the general anisotropy can be inspected. Note that the variations of propagation direction of guided waves are taken into account by rotating the crystallographic axes. Consequently, the latter submatrices can be full in many cases.

2.2 Fluid media

To simplify the calculation developments, mainly to express the state vector in a fluid that will be introduced later, it is of interest to express the fields and equations under consideration by using the displacement and velocity potentials. Thus, all the fields are derived from the displacement potential $\psi(z)$ satisfying the following ordinary differential equation:

$$\psi''(z) = \left(k^2 + \nu^2 - \frac{\omega^2}{c^2} \right) \psi(z), \quad (3)$$

where c denotes the uniform sound speed.

Indeed, the velocity potential $\phi(z)$, the displacement vector $\mathbf{u}(z)$ and the acoustic pressure $p(z)$ are defined as follows:

$$\phi(z) = \mathfrak{i} \omega \psi(z), \quad \mathbf{u}(z) = \begin{bmatrix} -\mathfrak{i} k \psi(z) \\ -\mathfrak{i} \nu \psi(z) \\ \psi'(z) \end{bmatrix} \quad \text{and} \quad p(z) = \rho \omega^2 \psi(z). \quad (4)$$

The expression of the acoustic pressure with respect to the displacement potential comes from Newton's second law, where ρ denotes the uniform mass density.

In the plate, Eqs. (1) and (2) in solid layers and Eqs. (3) and (4) in fluid layers will be directly included in the numerical scheme without being solved, as shown below.

¹The case of a fluid layer bounded by a rigid wall is also treated in the appendices.

In contrast, in any fluid half-space loading the plate, it must be specified that the searched wave of vertical wavenumber κ_α is only one of the two possible waves with opposite vertical wavenumbers, where

$$\kappa_\alpha = \pm \sqrt{\frac{\omega^2}{c_\alpha^2} - k^2 - \nu^2}, \quad \alpha = u, \ell. \quad (5)$$

The subscripts u and ℓ denote the upper ($z < 0$) and lower ($z > \ell$) half-spaces, respectively.

Each field $f(z)$ in a fluid half-space ($f = \psi, \phi, p, \mathbf{u}, \dots$) is analytically expressed by:

$$f(z) = f_u \exp(i \kappa_u z), \quad z < 0, \quad \text{or} \quad f(z) = f_\ell \exp[i \kappa_\ell (\ell - z)], \quad z > \ell, \quad (6)$$

in upper and lower half-spaces, respectively. Note that the wavenumbers κ_u and κ_ℓ correspond to opposite vertical directions to maintain the symmetry.

The main challenge below will be to deal with the square root expressions (5) of the vertical wavenumbers in the possible external fluids to build an eigenvalue problem that must be linear.

3 General equations obtained by discretization in the vertical direction

The final aim is to obtain an eigenvalue problem with respect to λ , in the classic form:

$$\lambda \mathbb{W} = \mathcal{G} \mathbb{W}, \quad (7)$$

where \mathbb{W} denotes a ‘‘global vector’’ that will entirely describe the fields in the discretized immersed plate and where the matrix \mathcal{G} is generated by the discretization of the equations summarized in the previous section. Three different cases are analyzed. For the first two cases, $\lambda = i \omega$ corresponds to the first derivative with respect to time t . These cases are the *fixed-wavenumber problem*, *i.e.*, it can be solved for a given wavenumber k , and the *fixed-slowness problem*, *i.e.*, it can be solved for a given slowness $s = k/\omega$. The third case is the *fixed-frequency problem*, the most widespread, where the frequency ω is given and $\lambda = -i k$ corresponds to the first derivative with respect to position x .

In this section, a set of equations, considered the last stage before obtaining the eigenvalue problem (7), is built by discretization in the vertical direction by using a high-order finite differences scheme.

3.1 Ordinary differential equation in each layer

In each layer, a ‘‘local state vector’’ $\mathbf{w}(z)$ must be defined such that the following ordinary differential system with respect to the vertical position z is satisfied:

$$\lambda \mathbf{w}(z) = M_0(z) \mathbf{w}(z) + M_1(z) \mathbf{w}'(z) + M_2(z) \mathbf{w}''(z). \quad (8)$$

The local state vector $\mathbf{w}(z)$ depends on the kind of medium. Typically, it is of dimension $d=6$ for a solid layer and of dimension $d=2$ for a fluid layer. It also depends on the type of *problem*, *i.e.*, *fixed-wavenumber*, *fixed-frequency* or *fixed-slowness*. For all possible cases, Table 1 gives the expressions of the local state vector as well as the associated subsections in the appendices where the specific expressions of the matrices $M_0(z)$, $M_1(z)$ and $M_2(z)$ can be found. The different components of state vectors $\mathbf{w}(z)$ are deduced from displacement fields $\mathbf{u}(z)$ for solid media, the solution of Eqs. (1) and (2), and from displacement potentials $\psi(z)$ for fluid media, the solution of Eq. (3).

It is very important to note that the choice of local state vectors is the key point of the method. Among all the possible state vectors, those that have been chosen make the initial goal possible, *i.e.*, the achievement of the desired eigenvalue problem. Other possibilities likely exist but have not been found. Generally, the

<i>Problem</i>	<i>Fixed-wavenumber</i>		<i>Fixed-frequency</i>		<i>Fixed-slowness</i>	
Searched eigenvalue	$\lambda = \mathbf{i} \omega$		$\lambda = -\mathbf{i} k$		$\lambda = \mathbf{i} \omega$	
Medium of the layer	Fluid	Solid	Fluid	Solid	Fluid	Solid
Local state vector $\mathbf{w}(z)$	$\begin{bmatrix} \phi(z) \\ p(z) \end{bmatrix}$	$\begin{bmatrix} \mathbf{u}(z) \\ \mathbf{v}(z)=\lambda \mathbf{u}(z) \end{bmatrix}$	$\begin{bmatrix} \psi(z) \\ u_x(z) \end{bmatrix}$	$\begin{bmatrix} \mathbf{u}(z) \\ \mathbf{v}(z)=\lambda \mathbf{u}(z) \end{bmatrix}$	$\begin{bmatrix} \phi(z) \\ p(z) \end{bmatrix}$	$\begin{bmatrix} \mathbf{u}(z) \\ \mathbf{v}(z)=\lambda \mathbf{u}(z) \end{bmatrix}$
Appendix	§ B.1	§ B.2	§ C.1	§ C.2	§ D.1	§ D.2

Table 1: Details on Eq. (8) with respect to both the treated *problem* and the medium: searched eigenvalues, local state vectors and section numbers in the appendices which give more details and the expressions of the matrix functions M_0 , M_1 and M_2 . Local state vector $\mathbf{w}(z)$ - Fluid: ψ , ϕ , p and u_x are the displacement and velocity potential, the acoustic pressure and the displacement in the x -direction. - Solid: $\mathbf{u}(z)$ is the displacement vector.

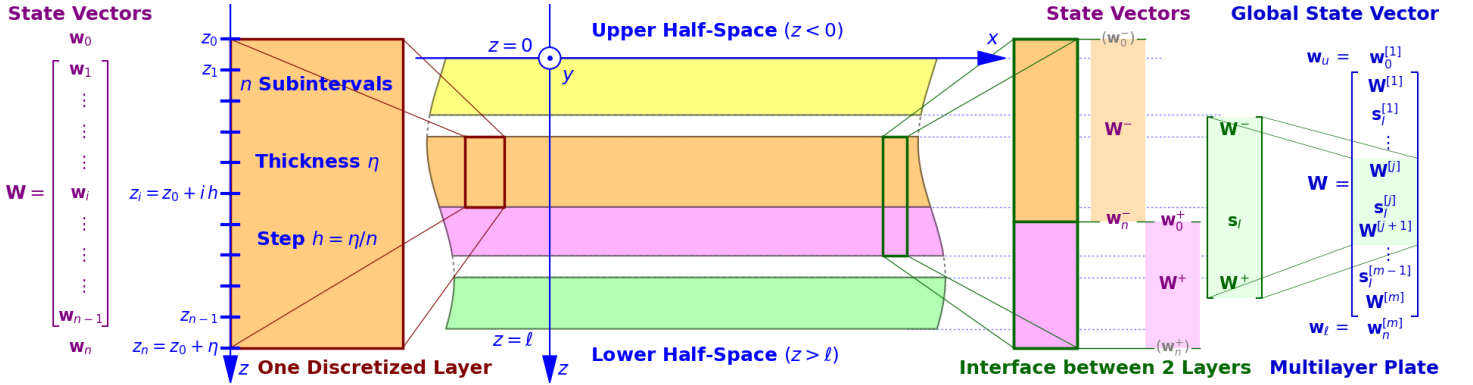


Figure 1: Geometry of the multilayer plate and state vectors. The discretization of each layer is described at the left-hand side, with the definition of the global state vector \mathbf{W} and local state vectors \mathbf{w}_0 and \mathbf{w}_n at the bounds. The right-hand side summarizes how an inner interface is taken into account in the global state vector of the plate by introducing the additional interfacial state vector \mathbf{s}_l .

definition of state vectors is a crucial point for many situations, *e.g.*, Stroh formalism [29] or the formulation of a biorthogonality relation for Lamb wave propagation [25].

To solve Eq. (8) for a single layer of thickness η , let us discretize the space with respect to the vertical position z into n subintervals of the same thickness $h = \eta/n$, to obtain $(n+1)$ vertical positions z_0, z_1, \dots, z_n , so-called the “nodes” of the mesh, as shown on the left side of Fig. 1. In doing so, we define a global state vector \mathbf{W} of dimension $(n-1) \times d$ containing the state vectors $\mathbf{w}(z_i)$, $i = 1, \dots, (n-1)$, at the inner nodes of the layer. By applying a high-order finite difference scheme, the following vectors \mathbf{W}' and \mathbf{W}'' approximate the vectors of first and second derivatives of the vector function \mathbf{w} at the inner nodes, respectively:

$$\mathbf{W}' = \frac{1}{h} (\mathcal{S}_1 \mathbf{w}_0 + \mathcal{D}_1 \mathbf{W} + \mathcal{T}_1 \mathbf{w}_n) \approx \begin{bmatrix} \mathbf{w}'(z_1) \\ \vdots \\ \mathbf{w}'(z_{n-1}) \end{bmatrix} \quad \text{and} \quad \mathbf{W}'' = \frac{1}{h^2} (\mathcal{S}_2 \mathbf{w}_0 + \mathcal{D}_2 \mathbf{W} + \mathcal{T}_2 \mathbf{w}_n) \approx \begin{bmatrix} \mathbf{w}''(z_1) \\ \vdots \\ \mathbf{w}''(z_{n-1}) \end{bmatrix}. \quad (9)$$

These approximations also depend on the two local state vectors $\mathbf{w}_0 = \mathbf{w}(z_0)$ and $\mathbf{w}_n = \mathbf{w}(z_n)$ at the upper and lower bounds, respectively. The newly introduced matrices \mathcal{S}_1 , \mathcal{D}_1 , \mathcal{T}_1 , \mathcal{S}_2 , \mathcal{D}_2 and \mathcal{T}_2 are given in A by

Eqs. (A.1) and (A.2). Finally, introducing the expressions (9) in the discretization of Eq. (8), leads to the following linear system:

$$\lambda \mathbf{W} = \mathcal{M} \mathbf{W} + \mathcal{C}_0 \mathbf{w}_0 + \mathcal{C}_n \mathbf{w}_n, \quad (10)$$

where:

$$\begin{cases} \mathcal{M} = \mathcal{M}_0 + \frac{1}{h} \mathcal{M}_1 \mathcal{D}_1 + \frac{1}{h^2} \mathcal{M}_2 \mathcal{D}_2 \\ \mathcal{C}_0 = \frac{1}{h} \mathcal{M}_1 \mathcal{S}_1 + \frac{1}{h^2} \mathcal{M}_2 \mathcal{S}_2 \\ \mathcal{C}_n = \frac{1}{h} \mathcal{M}_1 \mathcal{T}_1 + \frac{1}{h^2} \mathcal{M}_2 \mathcal{T}_2 \end{cases} \text{ and } \mathcal{M}_j = \begin{bmatrix} M_j(z_1) & \mathbb{O}_3 & \cdots & \cdots & \mathbb{O}_3 \\ \mathbb{O}_3 & M_j(z_2) & \ddots & & \vdots \\ \vdots & \ddots & \ddots & \ddots & \vdots \\ \vdots & & & \ddots & M_j(z_{n-2}) & \mathbb{O}_3 \\ \mathbb{O}_3 & \cdots & \cdots & \mathbb{O}_3 & M_j(z_{n-1}) \end{bmatrix}, \quad j = 0, 1, 2.$$

To go forward, the continuity at the interfaces between two layers will be taken into account in the next subsection.

3.2 Continuity at the internal interface of a bilayer

Eq. (10) holds true independently for any layer and contains the local state vectors \mathbf{w}_0 and \mathbf{w}_n at its upper and lower bounds. However, the local state vectors at each interface are coupled from one layer to another through the continuity equations. Let be an interface between two layers, for which all variables in the upper and lower layers are indexed by plus and minus, respectively. As shown on the right side of Fig. 1, the local state vectors \mathbf{w}_n^- and \mathbf{w}_0^+ are involved at this interface. The continuity of normal stress and of either displacement vector for solid/solid interfaces or vertical displacement for interfaces with at least one fluid provides complementary equations. These equations depend on the kind of interface and two cases must be analyzed separately.

On the one hand, for the simplest cases, the following linear systems at the interface can be written:

$$\mathbf{w}_n^- = \mathcal{K}_-^- \mathbf{W}^- + \mathcal{K}_-^+ \mathbf{W}^+ \quad \text{and} \quad \mathbf{w}_0^+ = \mathcal{K}_+^- \mathbf{W}^- + \mathcal{K}_+^+ \mathbf{W}^+. \quad (11)$$

The matrices \mathcal{K}_-^- , \mathcal{K}_-^+ , \mathcal{K}_+^- and \mathcal{K}_+^+ introduced in the generic form (11) depend on both the type of interface and the problem to solve. Their expressions are detailed in the appendices, and the link of each case with the corresponding subsection is given in Table 2. As an example, for the viscoelastic solid/viscoelastic solid interface and for the *fixed-wavenumber problem*, the matrices \mathcal{K}_-^- , \mathcal{K}_-^+ , \mathcal{K}_+^- and \mathcal{K}_+^+ can be easily identified from Eq. (B.17) in section B.4.3. This is a simple case, but other cases are more complicated, where the equations in the generic form (11) would be very large to display. Consequently, the interested reader can find such generic forms from the equations detailed in appendices.

Interface \ Problem	<i>Fixed-wavenumber</i>	<i>Fixed-frequency</i>	<i>Fixed-slowness</i> ²
Fluid/Fluid	§ B.4.1	§ C.4.1	§ D.4.1
Fluid/Solid	§ B.4.2	§ C.4.2	§ D.4.2
Solid/Solid	§ B.4.3	§ C.4.3	§ D.4.3

Table 2: Internal interfaces without or with [interfacial state vector](#), and subsection numbers in appendices indicate where they are detailed.

²For this problem, only the simple case of homogeneous fluids and homogeneous elastic solids is considered.

To fully take into account the interface equations, first, let us apply Eq. (10) to the two layers; second, replace \mathbf{w}_n^- and \mathbf{w}_0^+ in the latter two equations by their expression from Eq. (11) to obtain the following two equations:

$$\begin{aligned} \lambda \mathbf{W}^- &= \mathcal{C}_0^- \mathbf{w}_0^- + (\mathcal{M}^- + \mathcal{C}_n^- \mathcal{K}_-^-) \mathbf{W}^- + \mathcal{C}_n^- \mathcal{K}_-^+ \mathbf{W}^+ \quad \text{and} \\ \lambda \mathbf{W}^+ &= \mathcal{C}_0^+ \mathcal{K}_+^- \mathbf{W}^- + (\mathcal{C}_0^+ \mathcal{K}_+^+ + \mathcal{M}^+) \mathbf{W}^+ + \mathcal{C}_n^+ \mathbf{w}_n^+. \end{aligned} \quad (12)$$

On the other hand, more complicated cases exist, for which an additional equation at the interface must be satisfied. This is necessary because an **additional interfacial state vector** \mathbf{s}_I must be introduced to express the interface equations. Then, these equations can be written in the following generic linear system:

$$\begin{cases} \mathbf{w}_n^- = \mathcal{K}_-^- \mathbf{W}^- + \mathcal{K}_-^I \mathbf{s}_I + \mathcal{K}_-^+ \mathbf{W}^+ \\ \lambda \mathbf{s}_I = \mathcal{K}_I^- \mathbf{W}^- + \mathcal{K}_I^I \mathbf{s}_I + \mathcal{K}_I^+ \mathbf{W}^+ \\ \mathbf{w}_0^+ = \mathcal{K}_+^- \mathbf{W}^- + \mathcal{K}_+^I \mathbf{s}_I + \mathcal{K}_+^+ \mathbf{W}^+ \end{cases}, \quad (13)$$

where the new matrices \mathcal{K}_-^I , \mathcal{K}_I^- , \mathcal{K}_I^I , \mathcal{K}_I^+ and \mathcal{K}_+^I depend, once again, on both the type of interface and the problem dealt with. In Table 2, the link between each case and the corresponding subsection in the appendices can be found. The same processes as those used to obtain Eq. (12) can be applied to obtain the following three equations:

$$\begin{aligned} \lambda \mathbf{W}^- &= \mathcal{C}_0^- \mathbf{w}_0^- + (\mathcal{M}^- + \mathcal{C}_n^- \mathcal{K}_-^-) \mathbf{W}^- + \mathcal{C}_n^- \mathcal{K}_-^I \mathbf{s}_I + \mathcal{C}_n^- \mathcal{K}_-^+ \mathbf{W}^+, \\ \lambda \mathbf{s}_I &= \mathcal{K}_I^- \mathbf{W}^- + \mathcal{K}_I^I \mathbf{s}_I + \mathcal{K}_I^+ \mathbf{W}^+ \quad \text{and} \\ \lambda \mathbf{W}^+ &= \mathcal{C}_0^+ \mathcal{K}_+^- \mathbf{W}^- + \mathcal{C}_0^+ \mathcal{K}_+^I \mathbf{s}_I + (\mathcal{C}_0^+ \mathcal{K}_+^+ + \mathcal{M}^+) \mathbf{W}^+ + \mathcal{C}_n^+ \mathbf{w}_n^+. \end{aligned} \quad (14)$$

Finally, Eqs. (12) and (14), respectively, take the form:

$$\lambda \mathbf{W}_+^- = \mathcal{M}_+^- \mathbf{W}_+^- + \mathcal{C}_0^- \mathbf{w}_0^- + \mathcal{C}_n^+ \mathbf{w}_n^+, \quad \text{where } \mathbf{W}_+^- = \begin{bmatrix} \mathbf{W}^- \\ \mathbf{W}^+ \end{bmatrix} \quad \text{or} \quad \begin{bmatrix} \mathbf{W}^- \\ \mathbf{s}_I \\ \mathbf{W}^+ \end{bmatrix}, \quad (15)$$

stands for the state vector of the bilayer. At this stage, it is important to note that the above Eq. (15) exhibits the same form as Eq. (10). Consequently, from an algebraic point of view, through Eq. (15), a bilayer can be considered a single layer. This will be exploited in the next subsection to build the linear system associated with more general multilayer plates.

3.3 Final equation for multilayer plates

The system associated with the multilayer plate described in Fig. 1 is progressively built by taking the first layer and then adding the other layers one by one by using Eq. (15) to keep the same form (10) at each stage. At the end of the process, the following generic system can be written:

$$\lambda \mathbf{W} = \mathcal{M} \mathbf{W} + \mathcal{C}_u \mathbf{w}_u + \mathcal{C}_\ell \mathbf{w}_\ell, \quad (16)$$

where \mathbf{w}_u is the local state vector \mathbf{w}_0 of the first layer at its upper bound, and the vector \mathbf{w}_ℓ denotes the local state vector \mathbf{w}_n of the last layer at its lower bound. Of course, they cannot be eliminated for now. As a result, the system given in Eq. (16), unfortunately, does not exhibit the correct form introduced in Eq. (7) because the external boundary conditions are yet to be taken into account. This will be done in the next section.

To conclude, let us point out that other numerical methods, (*e.g.*, SAFE, TLM, and SBFEM) can very likely lead to the same formulation as Eq. (16), and, consequently, they can also be used in the process described in the next section.

4 Eigenvalue formulation for all possible cases

The goal is now to eliminate the two local state vectors \mathbf{w}_u and \mathbf{w}_ℓ at the plate bounds in Eq. (16). The process consists of expressing these two local state vectors as functions of both the global state vector \mathbf{W} and two possible **interfacial state vectors** \mathbf{s}_u and \mathbf{s}_ℓ by using the boundary conditions at the two external interfaces of the plate. These conditions depend on the medium, *i.e.*, solid or fluid, of the first and last plate layers and on the upper and lower half-spaces that are in contact with the plate. These external boundary conditions are exact.

With two half-spaces of either vacuum or fluid, four cases are possible: vacuum/vacuum, fluid/vacuum, fluid/fluid with a single fluid, or fluid/fluid with two different fluids. The much more complicated cases for which at least one of the two half-spaces is solid are not treated here because more than a single partial wave must be considered in a solid. This is still an open problem.

Writing the adequate equations requires a particular treatment for each *problem, i.e., fixed-wavenumber, fixed-frequency or fixed-slowness*. Details are given in the appendices. In Table 3, the link between the different cases and appendices can be found. Before giving details on calculation procedures, let us describe Table 3. It presents the state variables at the two external interfaces $z = 0$ and $z = \ell$. The two local state vectors in the first and last layers are denoted by $\mathbf{w}_u = \mathbf{w}(0^+)$ and $\mathbf{w}_\ell = \mathbf{w}(\ell^-)$, respectively. They are explicitly in agreement with Table 1. For particular external conditions and treated problems, **interfacial state vectors**, denoted by \mathbf{s}_u and \mathbf{s}_ℓ , must be introduced. For further investigations, let r_u and r_ℓ be the dimensions of the vectors \mathbf{s}_u and \mathbf{s}_ℓ , respectively. Each interfacial vector is expressed from different fields in the external half-space if it is of fluid, and in both the external layer and the external half-space if it is solid. This vector can be empty, *e.g.*, for a fluid layer in contact with a half-space of vacuum. In contrast, its maximum dimension is $2 + 2r$ where r is the rank of the stiffness matrix \mathcal{C}_{zx} of the solid layer at its external side.

The next subsections describe how it is possible to obtain eigenvalue formulations for the four cases mentioned above. Even if it is a specific case, the authors encourage the reader to first analyze § C.3.3, which concerns the vacuum/viscoelastic solid interface. Generic equations for solid media are fully detailed only in this subsection.

4.1 Plate in vacuum

For this well-known case, the following two generic equations can be formulated by rewriting the boundary conditions at $z = 0$:

$$\lambda \mathbf{s}_u = \mathcal{M}_u \mathbf{s}_u + \mathcal{N}_u \mathbf{W} \quad \text{and} \quad \mathbf{w}_u = \mathcal{Q}_u \mathbf{s}_u + \mathcal{R}_u \mathbf{W}, \quad (17)$$

where an **interfacial state vector** \mathbf{s}_u has been introduced, as detailed for different cases in subsections referenced in Table 3. Follow the links given in Table 3 to obtain for each case the expressions of the \mathbf{s}_u vector and of matrices \mathcal{M}_u , \mathcal{N}_u , \mathcal{Q}_u and \mathcal{R}_u . It is noticeable that the rectangular matrices \mathcal{N}_u and \mathcal{R}_u are sparse and contain nonzero coefficients only in their first rows, which specifically correspond to the uppermost nodes of the first layer. These equations can include the simplest cases where the dimension of the interfacial state vector \mathbf{s}_u is zero and the matrices \mathcal{M}_u , \mathcal{N}_u and \mathcal{Q}_u are empty, which simply gives: $\mathbf{w}_u = \mathcal{R}_u \mathbf{W}$.

Similarly, a local state vector \mathbf{s}_ℓ at the interface $z = \ell$ is introduced such that:

$$\lambda \mathbf{s}_\ell = \mathcal{N}_\ell \mathbf{W} + \mathcal{M}_\ell \mathbf{s}_\ell \quad \text{and} \quad \mathbf{w}_\ell = \mathcal{R}_\ell \mathbf{W} + \mathcal{Q}_\ell \mathbf{s}_\ell. \quad (18)$$

Combining Eqs. (16), (17) and (18) immediately leads to the following set of equations after elimination of the state vectors \mathbf{w}_u and \mathbf{w}_ℓ :

$$\lambda \begin{pmatrix} \mathbf{s}_u \\ \mathbf{W} \\ \mathbf{s}_\ell \end{pmatrix} = \begin{pmatrix} \mathcal{M}_u & \mathcal{N}_u & \mathbb{O}_{r_u, r_\ell} \\ \mathcal{C}_u \mathcal{Q}_u & \mathcal{M} + \mathcal{C}_u \mathcal{R}_u + \mathcal{C}_\ell \mathcal{R}_\ell & \mathcal{C}_\ell \mathcal{Q}_\ell \\ \mathbb{O}_{r_\ell, r_u} & \mathcal{N}_\ell & \mathcal{M}_\ell \end{pmatrix} \begin{pmatrix} \mathbf{s}_u \\ \mathbf{W} \\ \mathbf{s}_\ell \end{pmatrix}, \quad (19)$$

where $\mathbb{O}_{n,m}$ denotes the n -by- m zero matrix. This system is a standard eigenvalue problem as introduced in Eq. (7). Its dimension is $(N+r_u+r_\ell)$, where N is the dimension of the global state vector \mathbf{W} .

Let us inspect the circumstances for which the interfacial state vectors \mathbf{s}_u and \mathbf{s}_ℓ are zero-dimensional vectors. Referring to Table 3, for the *fixed-wavenumber problem*, this occurs for any first and last layers. However, for the two other *problems*, this is only possible if the first and last layer are both fluid media. As a result, the system (19) is then reduced to: $\lambda \mathbf{W} = (\mathcal{M} + \mathcal{C}_u \mathcal{R}_u + \mathcal{C}_\ell \mathcal{R}_\ell) \mathbf{W}$.

To close this section, it is important to note that Eqs. (17) and (18), and therefore Eq. (19), hold true also for the *fixed-slowness problem* with external fluids, as shown in § D.3.4 and D.3.5 and summarized in Table 3. Consequently, the next sections are only applicable to *fixed-wavenumber* and *fixed-frequency problems*.

4.2 Plate in contact with an external fluid at one side only

Let us consider the plate in contact with an external fluid at $z = 0$ and free at $z = \ell$. Let us first deal with the free lower interface. Therefore, Eq. (16) can be rewritten by using Eq. (18). By doing so, the following incomplete eigenvalue problem is obtained:

$$\lambda \mathbf{W}^{[\ell]} = \mathcal{M}^{[\ell]} \mathbf{W}^{[\ell]} + \mathcal{C}_u^{[\ell]} \mathbf{w}_u, \text{ with } \mathbf{W}^{[\ell]} = \begin{pmatrix} \mathbf{W} \\ \mathbf{s}_\ell \end{pmatrix}, \mathcal{M}^{[\ell]} = \begin{pmatrix} \mathcal{M} + \mathcal{C}_\ell \mathcal{R}_\ell & \mathcal{C}_\ell \mathcal{Q}_\ell \\ \mathcal{N}_\ell & \mathcal{M}_\ell \end{pmatrix} \text{ and } \mathcal{C}_u^{[\ell]} = \begin{pmatrix} \mathcal{C}_u \\ \mathbb{D}_{r_\ell, N} \end{pmatrix}, \quad (20)$$

where the local state vector \mathbf{w}_ℓ is eliminated and the possible **interfacial state vector** \mathbf{s}_ℓ is included in the global state vector $\mathbf{W}^{[\ell]}$.

Much more complicated is the treatment of the external fluid in contact with the plate at $z = 0$ because the vertical wavenumber κ_u , defined by a square-root in Eq. (5), is a nonlinear expression of both the frequency ω

Problem		Fixed-wavenumber		Fixed-frequency		Fixed-slowness	
Medium of the first layer		Fluid	Solid	Fluid	Solid	Fluid	Solid
Local state vector \mathbf{w}_u		$\begin{bmatrix} \phi(0^+) \\ p(0^+) \end{bmatrix}$	$\begin{bmatrix} \mathbf{u}(0^+) \\ \mathbf{i} \omega \mathbf{u}(0^+) \end{bmatrix}$	$\begin{bmatrix} \psi(0^+) \\ u_x(0^+) \end{bmatrix}$	$\begin{bmatrix} \mathbf{u}(0^+) \\ -\mathbf{i} k \mathbf{u}(0^+) \end{bmatrix}$	$\begin{bmatrix} \phi(0^+) \\ p(0^+) \end{bmatrix}$	$\begin{bmatrix} \mathbf{u}(0^+) \\ \mathbf{i} \omega \mathbf{u}(0^+) \end{bmatrix}$
Additional interfacial state vector \mathbf{s}_u between the first layer and the upper half-space:	Vacuum	—	—	—	\mathbf{r}_0^\perp	—	\mathbf{r}_0^\perp
		§ B.3.2	§ B.3.3	§ C.3.2	§ C.3.3	§ D.3.2	§ D.3.3
	Fluid	$\begin{bmatrix} \phi_u \\ p_u \end{bmatrix}$	$\begin{bmatrix} \psi_u \\ \phi_u \\ p_u \\ v_{0z} \end{bmatrix}$	$\begin{bmatrix} \psi_u \\ u_{ux} \end{bmatrix}$	$\begin{bmatrix} \mathbf{r}_0^\perp \\ \mathbf{i} \kappa_u \mathbf{r}_0^\perp \\ \psi_u \\ u_{ux} \end{bmatrix}$	$\begin{bmatrix} \phi_u \end{bmatrix}$	\mathbf{r}_0^\perp
	§ B.3.4*	§ B.3.5*	§ C.3.4*	§ C.3.5*	§ D.3.4	§ D.3.5	

Table 3: State variables at the interface $z = 0$ and $z = \ell$. Local state vector at the upper external interface in the first layer $\mathbf{w}_u = \mathbf{w}(0^+)$, see Table 1. **Interfacial state vector** \mathbf{s}_u - External fluid dependence: ψ_u , ϕ_u , p_u and u_{ux} are the displacement and velocity potentials, the acoustic pressure and the displacement in the x -direction, respectively. They are expressed at $z = 0$. κ_u is the wavenumber in the z -direction, defined by Eq. (5). - Solid dependence: v_{0z} is the velocity in the z -direction. \mathbf{r}_0^\perp is a vector of dimension equal to the rank of the stiffness matrix \mathcal{C}_{zx} . To deal with the lower interface, replace \mathbf{w}_u by $\mathbf{w}_\ell = \mathbf{w}(\ell^-)$, and ψ_u , ϕ_u , p_u , u_{ux} , v_{0z} , κ_u and \mathbf{r}_0^\perp by ψ_ℓ , ϕ_ℓ , p_ℓ , $u_{\ell x}$, $v_{\ell z}$, $-\kappa_\ell$ and \mathbf{r}_ℓ^\perp . The equations at interfaces are given either by Eqs. (17) and (18) or by Eqs. (21) and (24). This last case is indicated by a star (*).

and the wavenumber k . Fortunately, the square of κ_u is a linear combination of both frequency and horizontal wavenumber squares. This property is essential for what follows, since the idea is to consider κ_u an additional unknown of a new eigenvalue problem. Anticipating the further eigenvalue formulation (22), this is the key point of this paper. In this spirit, the global state vector will be modified to include the vertical wavenumber κ_u , as done in [11] in a different way, leveraging the fact that we can find a convenient **interfacial state vector** \mathbf{s}_u such that:

$$\begin{aligned} \lambda \mathbf{s}_u &= \mathcal{M}_u \mathbf{s}_u + \mathcal{N}_u \mathbf{W} + \mathcal{P}_u (\mu_u \mathbf{W}) , & (a) \\ \mathbf{w}_u &= \mathcal{Q}_u \mathbf{s}_u + \mathcal{R}_u \mathbf{W} + \mathcal{S}_u (\mu_u \mathbf{W}) \text{ and} & (b) \\ (\mu_u \mathbf{w}_u) &= \mathcal{T}_u \mathbf{s}_u + \mathcal{U}_u \mathbf{W} + \mathcal{V}_u (\mu_u \mathbf{W}) , & (c) \end{aligned} \quad (21)$$

with the new parameter $\mu_u = \mathfrak{i} \kappa_u$, as λ denotes either $\mathfrak{i} \omega$ or $-\mathfrak{i} k$. To our knowledge, this kind of technique has been used only by Hiyashi and Inoue [11] for the *fixed-frequency problem*, with a semi-analytical finite element method and more complex calculations. At this stage, it is of great interest to put emphasis on the essence of the method. As a matter of fact, it is particularly delicate to find the convenient **interfacial state vector** \mathbf{s}_u because Eq. (21) contains both **additional terms at the right-hand side** with respect to Eq. (17) and **an additional equation at its third row** involving the new state vector components $(\mu_u \mathbf{w}_u)$ and $(\mu_u \mathbf{W})$. Note that all matrices introduced in Eq. (21), *i.e.*, $\mathcal{M}_u, \mathcal{N}_u, \mathcal{P}_u, \mathcal{Q}_u, \mathcal{R}_u, \mathcal{S}_u, \mathcal{T}_u, \mathcal{U}_u$ and \mathcal{V}_u , do not depend on the parameter μ_u . These matrices depend on the first layer medium, *i.e.* fluid or solid, in contact with the upper external fluid and on the treated *problem*. The expressions of these matrices can be found in the appendices referenced in Table 3. It is important to note that the **interfacial state vector** \mathbf{s}_u is always necessary when the external interface is not free, as indicated in Table 3. It is different from the possible interfacial state vector \mathbf{s}_u at an interface with vacuum used in the previous section.

Our primary goal is now achieved. Indeed, Eqs. (20) and (21) lead to the following eigenvalue problem as written in Eq. (7):

$$\lambda \underbrace{\begin{bmatrix} \mathbf{s}_u \\ \mathbf{W}^{[\ell]} \\ (\mu_u \mathbf{W}^{[\ell]}) \end{bmatrix}}_{\mathbb{W}} = \underbrace{\begin{pmatrix} \mathcal{M}_u & \mathcal{N}_u^{[\ell]} & \mathcal{P}_u^{[\ell]} \\ \mathcal{C}_u^{[\ell]} \mathcal{Q}_u & \mathcal{M}^{[\ell]} + \mathcal{C}_u^{[\ell]} \mathcal{R}_u^{[\ell]} & \mathcal{C}_u^{[\ell]} \mathcal{S}_u^{[\ell]} \\ \mathcal{C}_u^{[\ell]} \mathcal{T}_u & \mathcal{C}_u^{[\ell]} \mathcal{U}_u^{[\ell]} & \mathcal{M}^{[\ell]} + \mathcal{C}_u^{[\ell]} \mathcal{V}_u^{[\ell]} \end{pmatrix}}_{\mathcal{G}} \underbrace{\begin{bmatrix} \mathbf{s}_u \\ \mathbf{W}^{[\ell]} \\ (\mu_u \mathbf{W}^{[\ell]}) \end{bmatrix}}_{\mathbb{W}}, \quad (22)$$

of dimension $[r_u + 2(N + r_\ell)]$ and where $\mathcal{Z}_u^{[\ell]} = (\mathcal{Z}_u \oplus_{r_\ell, r_\ell})$, $\mathcal{Z} \in \{\mathcal{N}, \mathcal{P}\}$, are r_ℓ -by- $(N + r_\ell)$ matrices and $\mathcal{Z}_u^{[\ell]} = (\mathcal{Z}_u \oplus_{N, r_\ell})$, $\mathcal{Z} \in \{\mathcal{R}, \mathcal{S}, \mathcal{U}, \mathcal{V}\}$, are N -by- $(N + r_\ell)$ matrices. All of these matrices are defined such that $\mathcal{Z}_u \mathbf{W} = \mathcal{Z}_u^{[\ell]} \mathbf{W}^{[\ell]}$. The third component $(\mu_u \mathbf{W}^{[\ell]})$ of the global state vector \mathbb{W} is the mean to take into account the vertical wavevector in the external fluid without using its expression (5). This kind of technique is well-known to transform a second-order scalar ordinary differential equation (ODE) into a first-order vector ODE or in Stroh formalism [29]. The **first row** of the global matrix \mathcal{G} is directly obtained by using Eq. (21.a). The second row of \mathcal{G} is built by replacing the local state vector \mathbf{w}_u in Eq. (20) by its expression (21.b). The **last row** of \mathcal{G} results from the product of Eq. (20) by μ_u , in which $(\mu_u \mathbf{w}_u)$ is then replaced by its expression (21.c).

4.3 Plate in contact with two external fluids with the same sound speed

If the plate is in contact with external fluids at both sides, we begin by the elimination of the local state vector \mathbf{w}_u at $z = 0$, as explained above to obtain Eq. (22), except that in this case, Eq. (20) is replaced by Eq. (16) while Eq. (21) remains used. Doing so provides the following system:

$$\lambda \underbrace{\begin{pmatrix} \mathbf{s}_u \\ \mathbf{W} \\ (\mu_u \mathbf{W}) \end{pmatrix}}_{\mathbb{W}^*} = \underbrace{\begin{pmatrix} \mathcal{M}_u & \mathcal{N}_u & \mathcal{P}_u \\ \mathcal{C}_u \mathcal{Q}_u & \mathcal{M} + \mathcal{C}_u \mathcal{R}_u & \mathcal{C}_u \mathcal{S}_u \\ \mathcal{C}_u \mathcal{T}_u & \mathcal{C}_u \mathcal{U}_u & \mathcal{M} + \mathcal{C}_u \mathcal{V}_u \end{pmatrix}}_{\mathcal{M}^*} \begin{pmatrix} \mathbf{s}_u \\ \mathbf{W} \\ (\mu_u \mathbf{W}) \end{pmatrix} + \underbrace{\begin{pmatrix} \mathbb{O}_{r_u, d_\ell} & \mathbb{O}_{r_u, d_\ell} \\ \mathcal{C}_\ell & \mathbb{O}_{N, d_\ell} \\ \mathbb{O}_{N, d_\ell} & \mathcal{C}_\ell \end{pmatrix}}_{\mathcal{C}_\ell^*} \underbrace{\begin{pmatrix} \mathbf{w}_\ell \\ (\mu_u \mathbf{w}_\ell) \end{pmatrix}}_{\mathbb{W}_\ell^*}, \quad (23)$$

where d_ℓ denotes the dimension of the local state vector \mathbf{w}_ℓ .

Thus, considering the vertical wavenumber $\kappa_\ell = -i\mu_\ell$ in the external fluid at the side $z = \ell$, we find a convenient state vector \mathbf{s}_ℓ such that:

$$\begin{aligned}\lambda \mathbf{s}_\ell &= \mathcal{M}_\ell \mathbf{s}_\ell + \mathcal{N}_\ell \mathbf{W} + \mathcal{P}_\ell (\mu_\ell \mathbf{W}) , \\ \mathbf{w}_\ell &= \mathcal{Q}_\ell \mathbf{s}_\ell + \mathcal{R}_\ell \mathbf{W} + \mathcal{S}_\ell (\mu_\ell \mathbf{W}) \text{ and} \\ \mu_\ell \mathbf{w}_\ell &= \mathcal{T}_\ell \mathbf{s}_\ell + \mathcal{U}_\ell \mathbf{W} + \mathcal{V}_\ell (\mu_\ell \mathbf{W}) .\end{aligned}\tag{24}$$

It is now necessary to separate the case where the two external fluids are identical, or at least have the same sound speed³, from the case where the sound speeds are different. This last case is treated in the next subsection. Each wavenumber κ_u or κ_ℓ corresponds to a single wave in each external fluid half-space. If the sound speeds are identical, these wavenumbers are either equal or opposite, *i.e.*, $\kappa_\ell = \varepsilon \kappa_u$ where $\varepsilon = \pm 1$. (i) If $\varepsilon = 1$, the wavevectors in the external fluids are symmetrical with respect to the plate plane. The plate is actually considered a waveguide. The two waves are either both outgoing or both ingoing. (ii) If $\varepsilon = -1$, the wavevectors are equal. The plate is crossed by the wave which is ingoing to one side and outgoing from the other side. With this notation, $\mu_\ell = \varepsilon \mu_u$ and combining Eqs. (23) and (24) gives the following eigenvalue problem of dimension $(r_u + 2N + r_\ell)$:

$$\lambda \begin{pmatrix} \mathbf{s}_u \\ \mathbf{W} \\ \mu_u \mathbf{W} \\ \mathbf{s}_\ell \end{pmatrix} = \begin{pmatrix} \mathcal{M}_u & \mathcal{N}_u & \mathcal{P}_u & \mathbb{D}_{r_u, r_\ell} \\ \mathcal{C}_u \mathcal{Q}_u & \mathcal{M} + \mathcal{C}_u \mathcal{R}_u + \mathcal{C}_\ell \mathcal{R}_\ell & \mathcal{C}_u \mathcal{S}_u + \varepsilon \mathcal{C}_\ell \mathcal{S}_\ell & \mathcal{C}_\ell \mathcal{Q}_\ell \\ \mathcal{C}_u \mathcal{T}_u & \mathcal{C}_u \mathcal{U}_u + \varepsilon \mathcal{C}_\ell \mathcal{U}_\ell & \mathcal{M} + \mathcal{C}_u \mathcal{V}_u + \mathcal{C}_\ell \mathcal{V}_\ell & \varepsilon \mathcal{C}_\ell \mathcal{T}_\ell \\ \mathbb{D}_{r_\ell, r_u} & \mathcal{N}_\ell & \varepsilon \mathcal{P}_\ell & \mathcal{M}_\ell \end{pmatrix} \begin{pmatrix} \mathbf{s}_u \\ \mathbf{W} \\ \mu_u \mathbf{W} \\ \mathbf{s}_\ell \end{pmatrix} .\tag{25}$$

Let us compare the solutions given by Hayashi and Inoue [11] and Kiefer *et al.* [18] with ours. Even if the essence of all is the same, the obtained final systems are different. This is notably because polynomial eigenvalue formulation is not used in the present paper. In addition, one of the most important reasons is that the specific state vectors have nothing to do with each other. Moreover, the assumptions of availability do not cover the same range of uses.

In that respect, an assumption of “*symmetry of Lamb wave modes under the conditions that leaky media are nonviscous fluids with the same sound velocities*” in anisotropic multilayered plates is made in [11] to obtain a third-order polynomial eigenvalue problem, which leads to an eigenvalue problem of dimension almost one and a half greater than the dimension of Eq. (25). A fourth-order polynomial eigenvalue problem is formulated in [18] by using a proper change of variables, as similarly done before in [13]. This latter “*procedure is applicable to anisotropic, viscoelastic, inhomogeneous, and layered plates coupled to an inviscid fluid*” and gives an eigenvalue problem of dimension approximately twice the dimension of Eq. (25). Thus, the smaller dimension of the eigenvalue problem (25) may have an appreciable impact on numerical computations. Furthermore, referring to the definitions given in the present paper, these two works deal only with the *fixed-frequency problem*. Another interest of the present approach is that inspecting a plate in contact with two different external fluids is just a matter of algebraic manipulations, as shown in the next subsection.

³assumption made in [11].

4.4 Plate in contact with two different external fluids

When the calculation architecture is well understood through the above examples, this last and more complicated case is easy to inspect. Skipping details, if the sound speeds in external fluids are different, Eqs. (23) and (24) lead to the following eigenvalue problem of dimension $(2r_u + 4N + 2r_\ell)$:

$$\lambda \begin{pmatrix} \mathbf{W}^* \\ \mu_\ell \mathbf{W}^* \\ \mathbf{s}_\ell^* \end{pmatrix} = \begin{pmatrix} \mathcal{M}^* + \mathcal{C}_\ell^* \mathcal{R}_\ell^* & \mathcal{C}_\ell^* \mathcal{S}_\ell^* & \mathcal{C}_\ell^* \mathcal{Q}_\ell^* \\ \mathcal{C}_\ell^* \mathcal{U}_\ell^* & \mathcal{M}^* + \mathcal{C}_\ell^* \mathcal{V}_\ell^* & \mathcal{C}_\ell^* \mathcal{T}_\ell^* \\ \mathcal{N}_\ell^* & \mathcal{P}_\ell^* & \mathcal{M}_\ell^* \end{pmatrix} \begin{pmatrix} \mathbf{W}^* \\ \mu_\ell \mathbf{W}^* \\ \mathbf{s}_\ell^* \end{pmatrix}, \quad (26)$$

where $\mathbf{s}_\ell^* = \begin{pmatrix} \mathbf{s}_\ell \\ \mu_u \mathbf{s}_\ell \end{pmatrix}$, $\mathcal{M}_\ell^* = \begin{pmatrix} \mathcal{M}_\ell & \mathbb{O}_{r_\ell, r_\ell} \\ \mathbb{O}_{r_\ell, r_\ell} & \mathcal{M}_\ell \end{pmatrix}$, $\mathcal{Z}_\ell^* = \begin{pmatrix} \mathbb{O}_{r_\ell, r_u} & \mathcal{Z}_\ell & \mathbb{O}_{r_\ell, N} \\ \mathbb{O}_{r_\ell, r_u} & \mathbb{O}_{r_\ell, N} & \mathcal{Z}_\ell \end{pmatrix}$, $\mathcal{Z} \in \{\mathcal{N}, \mathcal{P}\}$,
 $\mathcal{Z}_\ell^* = \begin{pmatrix} \mathcal{Z}_\ell & \mathbb{O}_{d_\ell, r_\ell} \\ \mathbb{O}_{d_\ell, r_\ell} & \mathcal{Z}_\ell \end{pmatrix}$, $\mathcal{Z} \in \{\mathcal{Q}, \mathcal{T}\}$ and $\mathcal{Z}_\ell^* = \begin{pmatrix} \mathbb{O}_{d_\ell, r_\ell} & \mathcal{Z}_\ell & \mathbb{O}_{d_\ell, r_\ell} \\ \mathbb{O}_{d_\ell, r_\ell} & \mathbb{O}_{d_\ell, r_\ell} & \mathcal{Z}_\ell \end{pmatrix}$, $\mathcal{Z} \in \{\mathcal{R}, \mathcal{S}, \mathcal{U}, \mathcal{V}\}$.
All the other matrices are defined in Eq. (23).

5 Numerical results

This section reports some numerical results based on our numerical schemes. These results have been obtained by using an 8th-order finite difference scheme, detailed in A. The code has been carefully validated. First, the three separately formulated *problems* have been compared to each other for free plates and give the same results with a high-precision level for modes with real-valued eigenfrequencies and eigenwavenumbers, *i.e.*, attenuated neither in time nor in space. Second, regarding finite-element-like codes, convergence is checked by changing both discretization steps and order of the finite difference scheme. Thus, convergence is well controlled with respect to these two parameters.

Many computations have been done for comparison with the literature. Let us mention the analysis of such in the following cases: immersed monolayer isotropic plate by formulating an eigenvalue problem [11] or by using an iterative method [8]; and multilayer plate in vacuum with anisotropic and fluid layers [12]. All of these latter cases are *fixed-frequency problems*. The comparison has also been done with the *fixed-slowness problem* of an immersed isotropic plate [27]. All comparisons give similar dispersion curves.

Beyond these examples, more detailed investigations are shown in next three subsections for the three *problems* treated here. For all cases, these analyses concern a 1 mm thick brass plate. For the *fixed-frequency problem*, the plate is immersed in water, while for the other two *problems*, the plate is loaded by water on one side and by motor oil on the other side. Indeed, we focus on this latter example because to our knowledge, the case of two fluids with different sound speeds has never been addressed by solving an eigenvalue problem. For the *fixed-frequency* and *fixed-wavenumber problems*, modes can be obtained while the size of the global matrix is twice that of its dimension for plates immersed in a single fluid. In contrast, the *fixed-slowness problem* needs a global matrix of half-dimension, *i.e.*, of the same dimension as that for plates in vacuum. Material parameters are given in Table 4.

Material	Mass density	Compression sound speed	Shear sound speed
Brass *	$\rho_b = 8.44 \text{ mg}\cdot\text{mm}^{-3}$	$c_L = 4.475 \text{ mm}\cdot\mu\text{s}^{-1}$	$c_T = 2.204 \text{ mm}\cdot\mu\text{s}^{-1}$
Water *	$\rho_w = 1.00 \text{ mg}\cdot\text{mm}^{-3}$	$c_w = 1.48 \text{ mm}\cdot\mu\text{s}^{-1}$	—
Motor Oil \diamond	$\rho_o = 0.87 \text{ mg}\cdot\text{mm}^{-3}$	$c_o = 1.74 \text{ mm}\cdot\mu\text{s}^{-1}$	—

Table 4: Material parameters for computations, from [18] * and [8] \diamond .

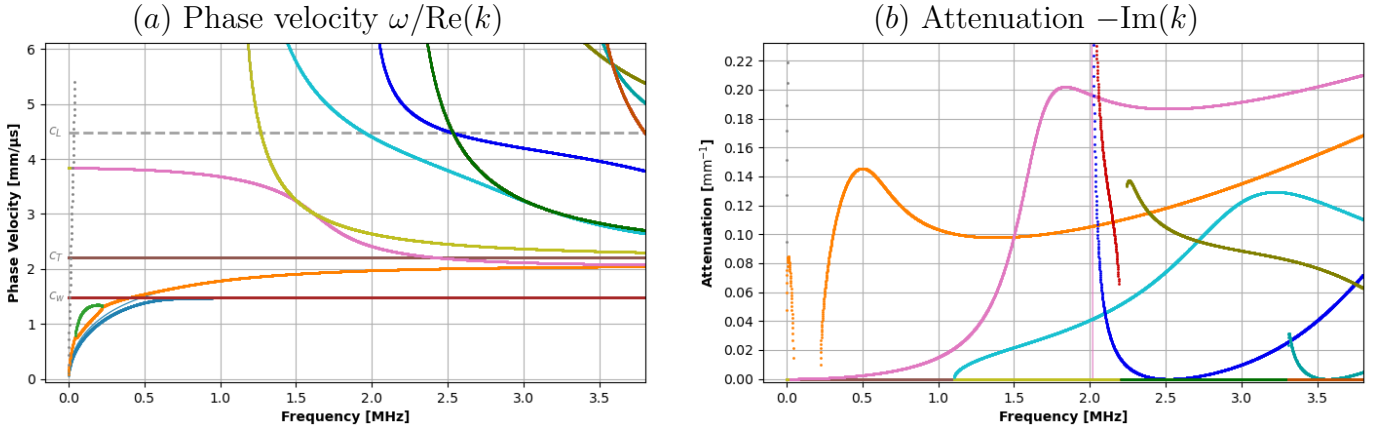


Figure 2: *Fixed-frequency problem* - 1 mm thick brass plate immersed in water: (a) phase velocities and (b) attenuations of modes versus frequency, to be compared with Fig. 7 of [18].

5.1 *Fixed-frequency problem*

For comparison with the recent article from Kiefer *et al.* [18], the example of the brass plate loaded by water at both sides is presented in Figure 2. This figure shows dispersion curves obtained for the *fixed-frequency problem*, where the phase velocity and attenuation are plotted versus the frequency. These curves overlap perfectly those of Fig. 7 from [18]. The dispersion curves of the SH modes, which are not attenuated because they do not interact with external fluids, appear in Figure 2, while they are not drawn in [18] because the present code treats general anisotropy without any simplifying assumption. To complete the comparison with this paper, let us note that for a plate loaded by water at one side only, *cf.* Fig. 5 of [18], similar results are obtained but not shown here.

5.2 *Fixed-wavenumber problem*

The dispersion curves obtained for the *fixed-wavenumber problem* are represented in Fig. 3a for the structure water/brass/motor oil. The wavenumber k is assumed to be real-valued. The complexity necessary to take into account the fluid loading is ensured by a complex frequency because attenuation is held by the imaginary part of the frequency. For comparison with the *fixed-frequency problem*, the associated attenuation is scaled with respect to position such that: $\text{Im}(\omega)/c_\varphi = k \text{Im}(\omega)/\text{Re}(\omega)$ where c_φ denotes the phase velocity. This normalized attenuation is drawn on Fig. 3b. From a physical point of view, the subsonic modes at low frequencies might be interesting to be investigated more precisely, but this is out of the topic of the present paper.

This structure has not been shown for the *fixed-frequency problem* in the above subsection. Nevertheless, when comparing with the *fixed-wavenumber problem*, the dispersion curves are very close while the attenuations are different since they do not exhibit the same physical meaning. However, they have similar orders of magnitude, as observed in most cases. In the same spirit, the dispersion curves for the structure water/brass/water are not drawn in this section because they are close to the *fixed-frequency problem* drawn in Fig. 2. They are also similar to the case of the free plate, except for subsonic cases; see, *e.g.*, [28], *i.e.*, when the phase velocities are less than the sound speed c_w in water.

5.3 *Fixed-slowness problem*

Finally, Figure 4 shows the case where the slowness s , or the phase velocity $c_\phi = 1/s$, is fixed and real-valued. The structure is the same as in § 5.2. Let us first analyze the dispersion curves. They differ from the other two cases at low frequencies and for phase velocities lower than the sound speed c_o in oil, as shown in Fig. 4a. It must

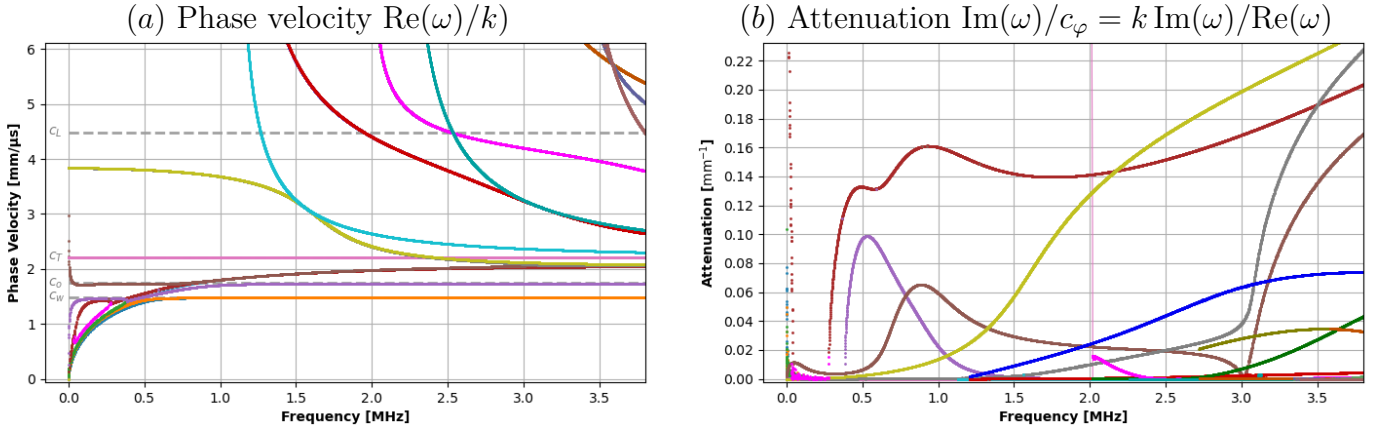


Figure 3: *Fixed-wavenumber problem* - water / 1 mm thick brass plate / motor oil: (a) phase velocities and (b) attenuations of modes versus frequency.

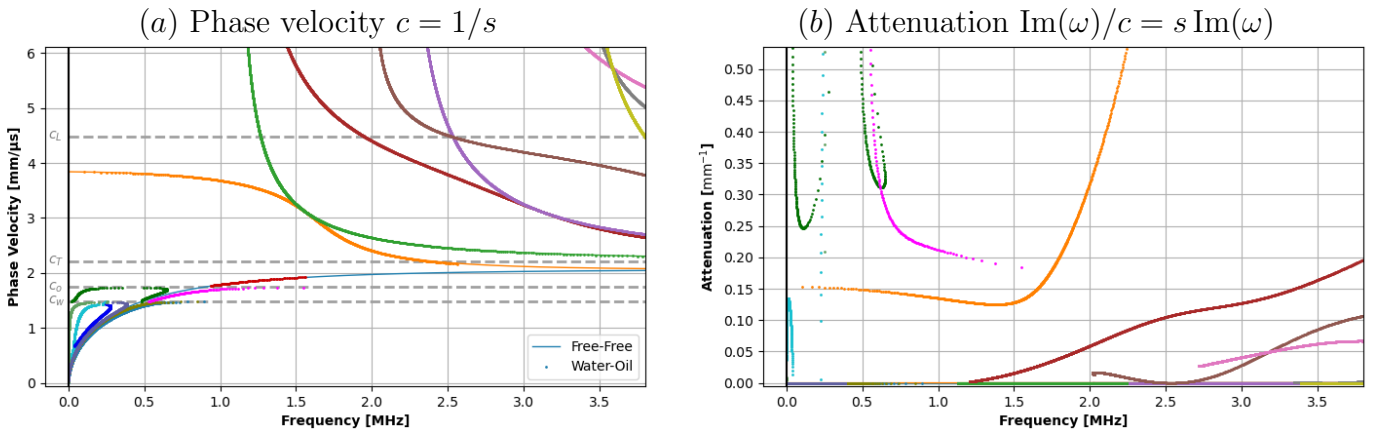


Figure 4: *Fixed-slowness problem* - water / 1 mm thick brass plate / motor oil: (a) phase velocities and (b) attenuations of modes versus frequency.

be noted that the computation of modes cannot be done if the phase velocity is in the close vicinity of any sound speed of any material, *i.e.*, c_L , c_T for brass, c_w for water and c_o . Indeed, the problem is necessarily ill-posed, exhibiting a singularity, because an infinity of modes should be found for phase velocity equal to c_T , c_w or c_o , as can be observed in Fig. 3 and shown in D for mathematical details. Second, let us examine the imaginary part of solutions, as illustrated in Fig. 4b, where $s \text{Im}(\omega) = \text{Im}(\omega)/c_\phi$ is drawn for comparing attenuations. The attenuations are notably different but in the same order of magnitude as the previous case. The amplitude of each attenuated mode is in this case both decreasing with respect to time at a given position and increasing with position at a given time; see [27] for more explanations.

6 Conclusion and prospects

A method has been developed to compute dispersion curves of guided waves for multilayered plates that exhibit no, one or two fluids loading one or two of its sides. This method, based on the formulation of an eigenvalue problem, provides a powerful and accurate tool that can be applied to any kind of layered material, *i.e.*, fluid, anisotropic and viscoelastic. To this end, interfacial state vectors must be introduced in certain situations at external and internal interfaces. This eigenvalue system can be formulated by fixing the frequency, the wavenumber or the slowness of the guided waves. These three formulations need matched treatments and correspond to three distinct meaningful problems that can be associated with three different physical models.

The method presented in this study is only applied to laminated plates immersed in fluids or not. However, it

seems possible to generalize this method to plates buried in isotropic elastic solids. At this stage, this is just an assumption that needs to be confirmed after additional efforts. Unfortunately, the generalization of this method to unidirectional waveguides of any section, as rods for instance, does not seem realistic. Restricting to circular multilayer pipes that satisfy the assumption of rotational invariance, it may be envisioned that this problem can be solved using the essence of our method. This is once again just a supposition.

Parallel to the present work, a study of energy velocities of elastic guided waves in immersed plates is in progress for the three problems associated with the three formulations.

References

- [1] A.V. Astaneh , M.N. Guddati (2015), *Efficient computation of dispersion curves for multilayered waveguides and half-spaces*, Comput. Methods Appl. Mech. Engrg. **300**, 27–46, DOI 10.1016/j.cma.2015.11.019.
- [2] M. Castaings, M. Lowe (2008), *Finite element model for waves guided along solid systems of arbitrary section coupled to infinite solid media*, J. Acous. Soc. Am. **123**(2), 696–708, DOI 10.1121/1.2821973.
- [3] É. Ducasse, M. Deschamps (2014), *Time-domain computation of the response of composite layered anisotropic plates to a localized source*, Wave Motion **51** (8), 1364–1381, DOI 10.1016/j.wavemoti.2014.08.003.
- [4] Z. Fan, M.J.S. Lowe, M. Castaings, C. Bacon (2008), *Torsional waves propagation along a waveguide of arbitrary cross section immersed in a perfect fluid*, J. Acoust. Soc. Am. **124**(4), 2002–2010, DOI 10.1121/1.2968677.
- [5] M. Gallezot, F. Treyssède, L. Laguerre (2017), *Contribution of leaky modes in the modal analysis of unbounded problems with perfectly matched layers*, J. Acoust. Soc. Am. **141** (1), Express Letters 16–21, DOI 10.1121/1.4973313.
- [6] L. Gavrić (1995), *Computation of propagative waves in free rail using a finite element technique*, J. Sound Vib. **185**, 531–543, DOI 10.1006/jsvi.1995.0398.
- [7] H. Gravenkamp, H. Man, C. Song, J. Prager (2013), *The computation of dispersion relations for three-dimensional elastic waveguides using the Scaled Boundary Finite Element Method*, J. Sound Vib. **332**, 3756–3771, DOI 10.1016/j.jsv.2013.02.007.
- [8] H. Gravenkamp, C. Birk, Ch. Song (2014), *Numerical modeling of elastic waveguides coupled to infinite fluid media using exact boundary conditions*, Computers and Structures **141**, 36–45, DOI 10.1016/j.compstruc.2014.05.010.
- [9] H. Gravenkamp, C. Birk, Ch. Song (2014), *Computation of dispersion curves for embedded waveguides using a dashpot boundary condition*, J. Acoust. Soc. Am. **135** (3), 1127–1138, DOI 10.1121/1.4864303.
- [10] H. Gravenkamp, C. Birk, J. Van (2015), *Modeling ultrasonic waves in elastic waveguides of arbitrary cross-section embedded in infinite solid medium*, Computers and Structures **149**, 61–71, DOI 10.1016/j.compstruc.2014.11.007.
- [11] T. Hayashi, D. Inoue (2014), *Calculation of leaky Lamb waves with a semi-analytical finite element method*, Ultrasonics **54**, 1460–1469. DOI 10.1016/j.ultras.2014.04.021.
- [12] F. Hernando Quintanilla, M.J.S. Lowe, R.V. Craster (2015), *Modeling guided elastic waves in generally anisotropic media using a spectral collocation method*, J. Acous. Soc. Am. **137**, 1180–1194, DOI 10.1121/1.4913777.
- [13] A. C. Hladky-Hennion, P. Langlet, R. Bossut, M. De Billy (1998), *Finite element modelling of radiating waves in immersed wedges*, J. Sound Vib. **212** (2), 265–274, DOI 10.1006/jsvi.1997.1408.

-
- [14] E. Kausel (1986), *Wave Propagation in Anisotropic Layered Media*, Int. J. Num. Methods in Engineering **23**, 1567–1578, DOI 10.1002/nme.1620230811.
- [15] E. Kausel, J. Roësset J. (1992), *Frequency domain analysis of undamped systems*, J. Eng. Mech. **118**(4), 721–734, DOI 10.1061/(ASCE)0733-9399(1992)118:4(721).
- [16] A. Krishna, *Topological Imaging of Tubular Structures using Ultrasonic Guided Waves*, PhD Thesis, University of Bordeaux, defended in Sept. 2020. 2020BORD0111.
- [17] E. Kausel (1994), *Thin-Layer Method: formulation in the time domain*, Int. J. Numer. Meth. Eng. **37** (6), 927–941, DOI 10.1002/nme.1620370604.
- [18] D. A. Kiefer, M. Ponschab, S. J. Rupitsch, M. Mayle (2019), *Calculating the full leaky Lamb wave spectrum with exact fluid interaction*, J. Acous. Soc. Am. **145**(6), 3341–3350, DOI 10.1121/1.5109399.
- [19] M. Lowe (1995), *Matrix techniques for modeling ultrasonic waves in multilayered media*, IEEE Transactions on Ultrasonics, Ferroelectrics and Frequency Control **42** (4), 525–542, DOI 10.1109/58.393096.
- [20] M. Mazzotti, I. Bartoli, A. Marzani, E. Viola (2013); *A coupled SAFE–2.5D BEM approach for the dispersion analysis of damped leaky guided waves in embedded waveguides of arbitrary cross-section*, Ultrasonics **53**, 1227–1241, DOI 10.1016/j.ultras.2013.03.003.
- [21] M. Mazzotti, A. Marzani, I. Bartoli (2014), *Dispersion analysis of leaky guided waves in fluid-loaded waveguides of generic shape*, Ultrasonics **54** (1), 408–418, DOI 10.1016/j.ultras.2013.06.011.
- [22] P. Mora, É. Ducasse, M. Deschamps (2016), *Transient 3D elastodynamic field in an embedded multilayered anisotropic plate*, Ultrasonics **69**, 106–115, DOI 10.1016/j.ultras.2016.03.020.
- [23] K.L. Nguyen, F. Treyssède, C. Hazard (2015), *Numerical modeling of three-dimensional open elastic waveguides combining semi-analytical finite element and perfectly matched layer methods*, J. Sound Vib. **344**, 158–178, DOI /10.1016/j.jsv.2014.12.032.
- [24] V. Pagneux, A. Maurel (2001), *Determination of Lamb mode eigenvalues*, J. Acous. Soc. Am. **110**, 1307–14, DOI 10.1121/1.1391248.
- [25] V. Pagneux, A. Maurel (2002), *Lamb wave propagation in inhomogeneous elastic waveguides*, Proc. R. Soc. Lond. A. **458**, 1913–1930, DOI 10.1098/rspa.2001.0950.
- [26] B. Pavlakovic, M.J.S. Lowe, D.N. Alleyne, P. Cawley (1997), *Disperse: a general purpose program for creating dispersion curves*, in: D.O. Thompson, D.E. Chimenti (Eds.), Review of Progress in Quantitative NDE **16**, Plenum Press, New York, 1997, 185–192, DOI 10.1007/978-1-4615-5947-4_24.
- [27] O. Poncelet, M. Deschamps (1997), *Lamb waves generated by complex harmonic inhomogeneous plane waves*, J. Acous. Soc. Am. **102**, 292–300, DOI 10.1121/1.419752.
- [28] A. Shuvalov, O. Poncelet, M. Deschamps (2005), *Analysis of the dispersion spectrum of fluid-loaded anisotropic plates: flexural-type branches and real-valued loops*, J. Sound Vib. **290**, 1175–1201, DOI 10.1016/j.jsv.2005.05.015.
- [29] A.N. Stroh (1962), *Steady state problems in anisotropic elasticity*, J. Math. Phys. **41**, 77–103, DOI 10.1002/sapm196241177.
- [30] F. Treyssède, K.L. Nguyen, A.-S. Bonnet-Ben Dhia, C. Hazard [2014], *Finite element computation of trapped and leaky elastic waves in open stratified waveguides*, Wave Motion **51** (7), 1093–1107, DOI 10.1016/j.wavemoti.2014.05.003.
- [31] P. Zuo, Z. Fan (2017), *SAFE–PML approach for modal study of waveguides with arbitrary cross sections immersed in inviscid fluid*, J. Sound Vib. **406**, 181–196, DOI 10.1016/j.jsv.2017.06.001.

A Finite differences in vertical position z

Let us discretize a layer of thickness η in n slices of thickness $h = \eta/n$. The position of each inner node is $z_i = z_0 + i h$, $i = 1, 2, \dots, n-1$. To approximate a d -dimensional local state vector $\mathbf{w}(z)$ and its first and second derivatives, let us apply a finite difference scheme of $2m^{\text{th}}$ order on these three vectors. At position z_i , they are denoted by \mathbf{w}_i , \mathbf{w}'_i and \mathbf{w}''_i , respectively, such that $\mathbf{w}_i \approx \mathbf{w}(z_i)$, $\mathbf{w}'_i \approx \mathbf{w}'(z_i)$ and $\mathbf{w}''_i \approx \mathbf{w}''(z_i)$. Assuming that the number of slices satisfies $n > 2m + 2$ and noting $N = (n-1)d$, let us introduce the following N -dimensional vectors:

$$\mathbf{W} = \begin{pmatrix} \mathbf{w}_1 \\ \mathbf{w}_2 \\ \vdots \\ \mathbf{w}_{n-1} \end{pmatrix}, \quad \mathbf{W}' = \begin{pmatrix} \mathbf{w}'_1 \\ \mathbf{w}'_2 \\ \vdots \\ \mathbf{w}'_{n-1} \end{pmatrix} \quad \text{and} \quad \mathbf{W}'' = \begin{pmatrix} \mathbf{w}''_1 \\ \mathbf{w}''_2 \\ \vdots \\ \mathbf{w}''_{n-1} \end{pmatrix},$$

which express the approximations of the ‘‘global state vector’’ \mathbf{W} of the layer and its first and second derivatives at the inner discretization points of the interval $[0, \eta]$. An essential linear combination, associating the global state vector, its first derivative and the two local state vectors \mathbf{w}_0 and \mathbf{w}_n at the bounds of the layer, can be written as follows:

$$h \mathbf{W}' = \mathcal{S}_1 \mathbf{w}_0 + \mathcal{D}_1 \mathbf{W} + \mathcal{T}_1 \mathbf{w}_n, \quad (\text{A.1})$$

$$\text{where } \mathcal{S}_1 = \begin{pmatrix} d_{10}^{[1]} \mathbb{I}_d \\ d_{20}^{[1]} \mathbb{I}_d \\ \vdots \\ d_{m0}^{[1]} \mathbb{I}_d \\ \mathbb{O}_d \\ \vdots \\ \mathbb{O}_d \end{pmatrix}, \quad \mathcal{T}_1 = \begin{pmatrix} \mathbb{O}_d \\ \vdots \\ \mathbb{O}_d \\ -d_{m0}^{[1]} \mathbb{I}_d \\ \vdots \\ -d_{20}^{[1]} \mathbb{I}_d \\ -d_{10}^{[1]} \mathbb{I}_d \end{pmatrix} \quad \text{and} \quad \mathcal{D}_1 = \begin{pmatrix} \boxed{\mathcal{R}_{11}} & \mathbb{O}_d & \cdots & \cdots & \cdots & \mathbb{O}_d \\ \vdots & \vdots & \vdots & \vdots & & \vdots \\ \boxed{\mathcal{R}_{1m}} & \mathbb{O}_d & & & & \mathbb{O}_d \\ \boxed{\mathcal{R}_{1\text{cent}}} & \mathbb{O}_d & & & & \mathbb{O}_d \\ \mathbb{O}_d & \boxed{\mathcal{R}_{1\text{cent}}} & \mathbb{O}_d & & & \mathbb{O}_d \\ \vdots & \ddots & \ddots & \ddots & \ddots & \vdots \\ \mathbb{O}_d & \mathbb{O}_d & \boxed{\mathcal{R}_{1\text{cent}}} & \mathbb{O}_d & & \mathbb{O}_d \\ \mathbb{O}_d & & \mathbb{O}_d & \boxed{\mathcal{R}_{1\text{cent}}} & & \mathbb{O}_d \\ \mathbb{O}_d & & & \mathbb{O}_d & \boxed{\mathcal{R}_{1-m}} & \mathbb{O}_d \\ \vdots & & & \vdots & \vdots & \vdots \\ \mathbb{O}_d & \cdots & \cdots & \cdots & \mathbb{O}_d & \boxed{\mathcal{R}_{1-1}} \end{pmatrix}.$$

\mathcal{S}_1 and \mathcal{T}_1 are N -by- d matrices, while \mathcal{D}_1 is a N -square matrix. The matrices \mathcal{R}_{li} and \mathcal{R}_{1-i} , of dimension d -by- l with $l = 2md$, are such that:

$$\mathcal{R}_{li} = \begin{pmatrix} d_{i1}^{[1]} \mathbb{I}_d & d_{i2}^{[1]} \mathbb{I}_d & \cdots & d_{i2m}^{[1]} \mathbb{I}_d \end{pmatrix} \quad \text{and} \quad \mathcal{R}_{1-i} = \begin{pmatrix} -d_{i2m}^{[1]} \mathbb{I}_d & \cdots & -d_{i2}^{[1]} \mathbb{I}_d & -d_{i1}^{[1]} \mathbb{I}_d \end{pmatrix}.$$

The d -by- $(l+d)$ matrix $\mathcal{R}_{1\text{cent}} = \begin{pmatrix} d_{m0}^{[1]} \mathbb{I}_d & d_{m1}^{[1]} \mathbb{I}_d & \cdots & d_{m(2m-1)}^{[1]} \mathbb{I}_d & d_{m2m}^{[1]} \mathbb{I}_d \end{pmatrix}$ corresponds to the standard centered scheme. Due to the symmetry properties of the first derivative, the following relations hold true: $d_{m(2m-j)}^{[1]} = -d_{mj}^{[1]}$ for any index j , and therefore the central coefficient $d_{mm}^{[1]}$ is zero. Eq. (A.1) separates the physics components, *i.e.*, the state vectors, from the variables associated with the numeric scheme and included in the matrices \mathcal{S}_1 , \mathcal{T}_1 and \mathcal{D}_1 . In fact these matrices depend only on the coefficients $d_{ij}^{[1]}$ that come directly from the approximations of the first derivative. They are given in Table 5 for $m = 4$.

Similarly, the vector \mathbf{W}'' can be expressed as a linear combination of the global state vector \mathbf{W} and of the local state vectors \mathbf{w}_0 and \mathbf{w}_n such that:

$$h^2 \mathbf{W}'' = \mathcal{S}_2 \mathbf{w}_0 + \mathcal{D}_2 \mathbf{W} + \mathcal{T}_2 \mathbf{w}_n. \quad (\text{A.2})$$

\mathcal{S}_2 and \mathcal{T}_2 are N -by- d matrices, while \mathcal{D}_2 is an N -square matrix. This latter matrix is of the same form as the matrix \mathcal{D}_1 and contains the d -by- $(l+d)$ submatrices \mathcal{R}_{2i} and \mathcal{R}_{2-i} such that:

$$\mathcal{R}_{2i} = \begin{pmatrix} d_{i1}^{[2]} \mathbb{I}_d & d_{i2}^{[2]} \mathbb{I}_d & \cdots & d_{i(2m+1)}^{[2]} \mathbb{I}_d \end{pmatrix} \quad \text{and} \quad \mathcal{R}_{2-i} = \begin{pmatrix} d_{i(2m+1)}^{[2]} \mathbb{I}_d & \cdots & d_{i2}^{[2]} \mathbb{I}_d & d_{i1}^{[2]} \mathbb{I}_d \end{pmatrix}.$$

$d_{ij}^{[1]}$	u_0	u_1	u_2	u_3	u_4	u_5	u_6	u_7	u_8	u_9
u'_0	$-\frac{761}{280}$	8	-14	$\frac{56}{3}$	$-\frac{35}{2}$	$\frac{56}{5}$	$-\frac{14}{3}$	$\frac{8}{7}$	$-\frac{1}{8}$	
u'_1	$-\frac{1}{8}$	$-\frac{223}{140}$	$\frac{7}{2}$	$-\frac{7}{2}$	$\frac{35}{12}$	$-\frac{7}{4}$	$\frac{7}{10}$	$-\frac{1}{6}$	$\frac{1}{56}$	
u'_2	$\frac{1}{56}$	$-\frac{2}{7}$	$-\frac{19}{20}$	2	$-\frac{5}{4}$	$\frac{2}{3}$	$-\frac{1}{4}$	$\frac{2}{35}$	$-\frac{1}{168}$	
u'_3	$-\frac{1}{168}$	$\frac{1}{14}$	$-\frac{1}{2}$	$-\frac{9}{20}$	$\frac{5}{4}$	$-\frac{1}{2}$	$\frac{1}{6}$	$-\frac{1}{28}$	$\frac{1}{280}$	
u'_4	$\frac{1}{280}$	$-\frac{4}{105}$	$\frac{1}{5}$	$-\frac{4}{5}$	0	$\frac{4}{5}$	$-\frac{1}{5}$	$\frac{4}{105}$	$-\frac{1}{280}$	
u'_5		$\frac{1}{280}$	$-\frac{4}{105}$	$\frac{1}{5}$	$-\frac{4}{5}$	0	$\frac{4}{5}$	$-\frac{1}{5}$	$\frac{4}{105}$	$-\frac{1}{280}$
$d_{ij}^{[2]}$	u_0	u_1	u_2	u_3	u_4	u_5	u_6	u_7	u_8	u_9
u''_1	$\frac{761}{1260}$	$\frac{61}{144}$	$-\frac{201}{35}$	$\frac{341}{30}$	$-\frac{1163}{90}$	$\frac{411}{40}$	$-\frac{17}{3}$	$\frac{1303}{630}$	$-\frac{9}{20}$	$\frac{223}{5040}$
u''_2	$-\frac{223}{5040}$	$\frac{293}{280}$	$-\frac{395}{252}$	$-\frac{13}{30}$	$\frac{83}{40}$	$-\frac{319}{180}$	$\frac{59}{60}$	$-\frac{5}{14}$	$\frac{389}{5040}$	$-\frac{19}{2520}$
u''_3	$\frac{19}{2520}$	$-\frac{67}{560}$	$\frac{97}{70}$	$-\frac{89}{36}$	$\frac{23}{20}$	$\frac{7}{40}$	$-\frac{17}{90}$	$\frac{11}{140}$	$-\frac{1}{56}$	$\frac{1}{560}$
u''_4	$-\frac{1}{560}$	$\frac{8}{315}$	$-\frac{1}{5}$	$\frac{8}{5}$	$-\frac{205}{72}$	$\frac{8}{5}$	$-\frac{1}{5}$	$\frac{8}{315}$	$-\frac{1}{560}$	
u''_5		$-\frac{1}{560}$	$\frac{8}{315}$	$-\frac{1}{5}$	$\frac{8}{5}$	$-\frac{205}{72}$	$\frac{8}{5}$	$-\frac{1}{5}$	$\frac{8}{315}$	$-\frac{1}{560}$

Table 5: Finite difference coefficients $d_{ij}^{[1]}$ and $d_{ij}^{[2]}$ of the linear combinations linking the approximations u'_i and u''_i of the first and second derivatives of a function u at node $\#i$, respectively, to the values u_j of the function at nodes $\#j$, for an 8th order scheme.

The d -by- $(l+d)$ matrix $\mathcal{R}_{\text{cent}} = \begin{pmatrix} d_{m0}^{[2]} \mathbb{I}_d & d_{m1}^{[2]} \mathbb{I}_d & \cdots & d_{m(2m-1)}^{[2]} \mathbb{I}_d & d_{m2m}^{[2]} \mathbb{I}_d \end{pmatrix}$ is associated with the centered scheme and its coefficients satisfy the following symmetry property $d_{m(2m-j)}^{[2]} = d_{mj}^{[2]}$ for any index j . For a finite difference scheme of 8th order, the coefficients $d_{ij}^{[1]}$ and $d_{ij}^{[2]}$ associated with the first and second derivatives, respectively, are given in Table 5.

The first derivatives on the bounds of interval $[0, \eta]$ satisfy similar equations:

$$h \mathbf{w}'_0 = \ell_0 \mathbf{w}_0 + \mathcal{L}_0^{(d)} \mathbf{W} \quad \text{and} \quad h \mathbf{w}'_n = -\ell_0 \mathbf{w}_n + \mathcal{L}_n^{(d)} \mathbf{W}, \quad (\text{A.3})$$

with $\ell_0 = d_{00}^{[1]}$ and where the d -by- N matrices $\mathcal{L}_0^{(d)}$ and $\mathcal{L}_n^{(d)}$ are such that:

$$\mathcal{L}_0^{(d)} = \begin{pmatrix} d_{01}^{[1]} \mathbb{I}_d & \cdots & d_{0(2m)}^{[1]} \mathbb{I}_d & \mathbb{O}_d & \cdots & \mathbb{O}_d \end{pmatrix} \quad \text{and} \quad \mathcal{L}_n^{(d)} = \begin{pmatrix} \mathbb{O}_d & \cdots & \mathbb{O}_d & -d_{0(2m)}^{[1]} \mathbb{I}_d & \cdots & -d_{01}^{[1]} \mathbb{I}_d \end{pmatrix}.$$

The developed method considerably relies on the latter equations (A.3). For further investigations, the global state vector \mathbf{W} , containing the local state vectors \mathbf{w}_i defined in Table 1 for each case, will be separated into two global state subvectors by introducing one of the following three pairs: (Φ, \mathbf{P}) , (Ψ, \mathbf{U}_x) or (\mathbf{U}, \mathbf{V}) . These notations will be useful in the next three appendices.

B Detailed calculations for the *fixed-wavenumber problem*

B.1 Local state vector in homogeneous fluid [Eq. (8), Table 1]

The chosen local state vector is two-dimensional, consisting of the velocity potential and acoustic pressure components. Therefore, by using Eqs. (3) and (4), the generic ODE (8) with respect to z is expressed with the following vector and matrices:

$$\mathbf{w}(z) = \begin{bmatrix} \phi(z) \\ p(z) \end{bmatrix}, \quad M_0 = \begin{bmatrix} 0 & -1/\rho \\ \rho c^2 (k^2 + \nu^2) & 0 \end{bmatrix}, \quad M_1 = \mathbb{O}_2 \quad \text{and} \quad M_2 = \begin{bmatrix} 0 & 0 \\ -\rho c^2 & 0 \end{bmatrix}. \quad (\text{B.1})$$

B.2 Local state vector in viscoelastic solid [Eq. (8), Table 1]

The local state vector is six-dimensional and contains the displacement and velocity vectors. From Eqs. (1) and (2), the generic ODE (8) is obtained with:

$$\mathbf{w}(z) = \begin{bmatrix} \mathbf{u}(z) \\ \mathbf{v}(z) = \mathbf{i} \omega \mathbf{u}(z) \end{bmatrix}, \quad M_0(z) = \begin{bmatrix} \mathbb{O}_3 & \mathbb{I}_3 \\ M_{021}(z) & M_{022}(z) \end{bmatrix}, \quad (\text{B.2})$$

$$M_1(z) = \begin{bmatrix} \mathbb{O}_3 & \mathbb{O}_3 \\ M_{121}(z) & M_{122}(z) \end{bmatrix} \quad \text{and} \quad M_2(z) = \begin{bmatrix} \mathbb{O}_3 & \mathbb{O}_3 \\ M_{221}(z) & M_{222}(z) \end{bmatrix},$$

with

$$\begin{cases} M_{021}(z) = \rho(z)^{-1} \{ -k^2 \mathcal{C}_{xx}(z) - k \nu [\mathcal{C}_{xy}(z) + \mathcal{C}_{yx}(z)] - \nu^2 \mathcal{C}_{yy}(z) - \mathbf{i} k \mathcal{C}'_{zx}(z) - \mathbf{i} \nu \mathcal{C}'_{zy}(z) \} \\ M_{022}(z) = \rho(z)^{-1} \{ -k^2 \mathcal{H}_{xx}(z) - k \nu [\mathcal{H}_{xy}(z) + \mathcal{H}_{yx}(z)] - \nu^2 \mathcal{H}_{yy}(z) - \mathbf{i} k \mathcal{H}'_{zx}(z) - \mathbf{i} \nu \mathcal{H}'_{zy}(z) \} \\ M_{121}(z) = \rho(z)^{-1} \{ -\mathbf{i} k [\mathcal{C}_{xz}(z) + \mathcal{C}_{zx}(z)] - \mathbf{i} \nu [\mathcal{C}_{yz}(z) + \mathcal{C}_{zy}(z)] + \mathcal{C}'_{zz}(z) \} \\ M_{122}(z) = \rho(z)^{-1} \{ -\mathbf{i} k [\mathcal{H}_{xz}(z) + \mathcal{H}_{zx}(z)] - \mathbf{i} \nu [\mathcal{H}_{yz}(z) + \mathcal{H}_{zy}(z)] + \mathcal{H}'_{zz}(z) \} \\ M_{221}(z) = \rho(z)^{-1} \mathcal{C}_{zz}(z) \\ M_{222}(z) = \rho(z)^{-1} \mathcal{H}_{zz}(z) \end{cases}.$$

B.3 External interface at $z = 0$

B.3.1 Rigid wall/homogeneous fluid [Eq. (17), Table 3]

For rigid walls, the boundary condition is such that the normal displacement is zero, *i.e.*, $\mathbf{w}'(0^+) = \mathbf{0}_2$. By using approximation Eq. (A.3), the state vector \mathbf{w}_u at the interface is immediately expressed with respect to the global state vector \mathbf{W} as follows: $\mathbf{w}_u = -(\ell_0)^{-1} \mathcal{L}_0^{(2)} \mathbf{W}$.

B.3.2 Vacuum/homogeneous fluid [Eq. (17), Table 3]

At a vacuum interface, both acoustic pressure and potentials are zero, *i.e.*, $\mathbf{w}(0^+) = \mathbf{w}_u = \mathbf{0}_2$.

B.3.3 Vacuum/viscoelastic solid [Eq. (17), Table 3]

For simplicity, we neglect viscosity at the interface, *i.e.*, all the matrices $\mathcal{H}_{\alpha\beta}(0^+)$, $\alpha, \beta = x, y, z$, in Eq. (2) are assumed to be zero. The normal stress at the interface satisfies: $\boldsymbol{\sigma}_z(0^+) = \mathbf{0}_3$. From Eq. (2) and approximation Eq. (A.3), the displacement vector \mathbf{u}_0 and the velocity vector \mathbf{v}_0 in the solid at the interface are given by: $\mathbf{u}_0 = \mathcal{A}_u \mathcal{L}_0^{(3)} \mathbf{U}$ and $\mathbf{v}_0 = \mathcal{A}_u \mathcal{L}_0^{(3)} \mathbf{V}$, where:

$$\mathcal{A}_u = \mathcal{B}_u \begin{bmatrix} \frac{1}{h} \mathcal{C}_{zz}(0^+) \end{bmatrix} \quad \text{with} \quad \mathcal{B}_u = \left\{ -\frac{\ell_0}{h} \mathcal{C}_{zz}(0^+) + \mathbf{i} [k \mathcal{C}_{zx}(0^+) + \nu \mathcal{C}_{zy}(0^+)] \right\}^{-1}. \quad (\text{B.3})$$

Note that the 3-by-3 matrix $\mathcal{C}_{zz}(z)$ is necessarily invertible. Consequently, the matrix \mathcal{B}_u is defined for a discretization step h small enough. Finally, the local state vector \mathbf{w}_u at the interface is a linear expression of the global state vector \mathbf{W} of the layer, as for the previous cases:

$$\mathbf{w}_u = \begin{pmatrix} \mathbf{u}_0 \\ \mathbf{v}_0 \end{pmatrix} = \begin{pmatrix} \mathcal{A}_u & \mathbb{O}_3 \\ \mathbb{O}_3 & \mathcal{A}_u \end{pmatrix} \mathcal{L}_0^{(6)} \mathbf{W}. \quad (\text{B.4})$$

The generic form (17) is then identified with Eq. (B.4) with an empty interfacial vector \mathbf{s}_u and empty matrices \mathcal{M}_u , \mathcal{N}_u and \mathcal{Q}_u .

B.3.4 Homogeneous fluid/homogeneous fluid [Eq. (21), Table 3]

From Eq. (6), the vertical velocity and acoustic pressure at $z = 0$ are such that: $\mathfrak{i} \kappa_u(k, \omega) \phi_u = \phi'(0^+)$ and $p_u = p(0^+)$, which implies $\rho_u \phi_u = \rho \phi(0^+)$. Using approximation Eq. (A.3), we deduce that:

$$\mathfrak{i} \kappa_u(k, \omega) \phi_u = \frac{1}{h} \left(\ell_0 \phi(0^+) + \mathcal{L}_0^{(1)} \Phi \right) \quad \text{and} \quad \mathfrak{i} \kappa_u(k, \omega) p_u = \frac{\rho_u}{\rho h} \left(\ell_0 p(0^+) + \mathcal{L}_0^{(1)} \mathbf{P} \right). \quad (\text{B.5})$$

To obtain an eigenvalue-like equation, let us express $\mathfrak{i} \omega p_u$ in the following form:

$$\begin{aligned} \mathfrak{i} \omega p_u &= \rho_u \omega^2 \phi_u = \rho_u c_u^2 [k^2 + \nu^2 + \kappa_u(k, \omega)^2] \phi_u \\ &= \rho_u c_u^2 \left\{ (k^2 + \nu^2) \phi_u - \mathfrak{i} \kappa_u(k, \omega) \left[\frac{1}{h} \left(\frac{\rho_u}{\rho} \ell_0 \phi_u + \mathcal{L}_0^{(1)} \Phi \right) \right] \right\}. \end{aligned}$$

Consequently, the components ϕ_u and p_u constituting the local state vector $\mathbf{w}(0^-)$ in the external fluid at the interface satisfy the following eigenvalue-like equations:

$$\begin{aligned} \mathfrak{i} \omega \phi_u &= -p_u / \rho_u \quad \text{and} \\ \mathfrak{i} \omega p_u &= \rho_u c_u^2 \left\{ \left[k^2 + \nu^2 - \left(\frac{\rho_u \ell_0}{\rho h} \right)^2 \right] \phi_u - \frac{\rho_u \ell_0}{\rho h^2} \mathcal{L}_0^{(1)} \Phi - \frac{1}{h} \mathcal{L}_0^{(1)} [\mathfrak{i} \kappa_u(k, \omega) \Phi] \right\}. \end{aligned} \quad (\text{B.6})$$

Both the local state vector $\mathbf{w}_u = \mathbf{w}(0^+)$ of the multilayer plate at the bound $z = 0$ and the vector $\mathfrak{i} \kappa_u(k, \omega) \mathbf{w}_u$ can be expressed as follows:

$$\mathbf{w}_u = \begin{pmatrix} \rho_u / \rho & 0 \\ 0 & 1 \end{pmatrix} \mathbf{w}(0^-) \quad \text{and} \quad \mathfrak{i} \kappa_u(k, \omega) \mathbf{w}_u = \frac{\rho_u}{\rho h} \left[\ell_0 \begin{pmatrix} \rho_u / \rho & 0 \\ 0 & 1 \end{pmatrix} \mathbf{w}(0^-) + \mathcal{L}_0^{(2)} \mathbf{W} \right]. \quad (\text{B.7})$$

Considering the **additional interfacial state vector** $\mathbf{s}_u = \mathbf{w}(0^-)$, from Eqs. (B.6) and (B.7), the system (21) is completely defined.

B.3.5 Homogeneous fluid/viscoelastic solid [Eq. (21), Table 3]

Continuity of both vertical velocity and acoustic pressure at $z = 0$ leads to: $\mathfrak{i} \kappa_u(k, \omega) \phi_u = v_z(0^+)$ and $p_u \mathbf{n} = -\boldsymbol{\sigma}_z(0^+) = \mathfrak{i} [k \mathcal{C}_{zx}(0^+) + \nu \mathcal{C}_{zy}(0^+)] \mathbf{u}(0^+) - \mathcal{C}_{zz}(0^+) \mathbf{u}'(0^+)$, where \mathbf{n} denotes the unit vector in the z -direction. From approximation Eq. (A.3) and definition (B.3), we obtain the displacement vector \mathbf{u}_0 in the solid at the interface, with respect to the acoustic pressure p_u in the fluid at the interface and the global displacement vector \mathbf{U} inside the solid:

$$\mathbf{u}_0 = p_u \mathcal{B}_u \mathbf{n} + \mathcal{A}_u \mathcal{L}_0^{(3)} \mathbf{U}. \quad (\text{B.8})$$

After some algebra, it seems convenient to consider the four-dimensional interfacial state vector \mathbf{s}_u in the external fluid at the interface, whose components are the acoustic pressure p_u , the velocity potential ϕ_u , the displacement potential ψ_u and the velocity v_{0z} in the z -direction. Indeed, we obtain the following eigenvalue-like equations:

$$\begin{aligned} \mathfrak{i} \omega p_u &= \frac{1}{\beta_u} (v_{0z} - \mathbf{a}_u \cdot \mathbf{V}) , \quad \mathfrak{i} \omega \psi_u = \phi_u , \\ \mathfrak{i} \omega \phi_u &= -\frac{1}{\rho_u} p_u \quad \text{and} \quad \mathfrak{i} \omega v_{0z} = \frac{1}{\beta_u \rho_u} \left\{ \frac{p_u}{\rho_u c_u^2} - (k^2 + \nu^2) \psi_u + \mathbf{a}_u \cdot [\mathfrak{i} \kappa_u(\omega, k) \mathbf{U}] \right\} , \end{aligned} \quad (\text{B.9})$$

where the vector \mathbf{a}_u is the last row of the matrix $\mathcal{A}_u \mathcal{L}_0^{(3)}$ and the non-zero coefficient β_u is the (3, 3)-component of the matrix \mathcal{B}_u . To express the local state vector \mathbf{w}_u at the interface defined by Eq. (B.2), let us complete Eq. (B.8) by expressing the velocity vector \mathbf{v}_0 as follows:

$$\mathbf{v}_0 = v_{0z} \mathbf{n} + \mathbb{J} \mathcal{A}_u \mathcal{L}_0^{(3)} \mathbf{V} , \quad \text{where } \mathbb{J} = \begin{pmatrix} 1 & 0 & 0 \\ 0 & 1 & 0 \\ 0 & 0 & 0 \end{pmatrix} . \quad (\text{B.10})$$

Combining the square of Eq. (5) and Eqs. (B.9) and (B.10) yields the following expressions of the vectors $[\mathfrak{i} \kappa_u(k, \omega) \mathbf{u}_0]$ and $[\mathfrak{i} \kappa_u(k, \omega) \mathbf{v}_0]$:

$$\begin{aligned} \mathfrak{i} \kappa_u(k, \omega) \mathbf{u}_0 &= \left[(k^2 + \nu^2) \psi_u - \frac{p_u}{\rho_u c_u^2} \right] \mathbf{n} + \mathbb{J} \mathcal{A}_u \mathcal{L}_0^{(3)} [\mathfrak{i} \kappa_u(k, \omega) \mathbf{U}] \quad \text{and} \\ \mathfrak{i} \kappa_u(k, \omega) \mathbf{v}_0 &= \left[(k^2 + \nu^2) \phi_u + \frac{1}{\beta_u \rho_u c_u^2} (\mathbf{a}_u \cdot \mathbf{V} - v_{0z}) \right] \mathbf{n} + \mathbb{J} \mathcal{A}_u \mathcal{L}_0^{(3)} [\mathfrak{i} \kappa_u(k, \omega) \mathbf{V}] . \end{aligned} \quad (\text{B.11})$$

Consequently, the local state vector \mathbf{w}_u is expressed in Eqs. (B.8) and (B.10) with respect to both the two global state vectors \mathbf{W} and $[\mathfrak{i} \kappa_u(k, \omega) \mathbf{W}]$ and the components of the interfacial state vector \mathbf{s}_u that satisfies the eigenvalue-like system (B.9). With Eq. (B.11), the generic system (21) is then totally defined.

B.4 Internal interfaces

B.4.1 Homogeneous fluid/homogeneous fluid [Eq. (11), Table 2]

Continuity of vertical velocity and acoustic pressure at $z = z_I$ leads to: $(\phi^-)'(z_I^-) = (\phi^+)'(z_I^+)$ and $p^-(z_I^-) = p^+(z_I^+)$. From these equations and approximation Eq. (A.3), we deduce that: $p_n^- = p_0^+$, $\rho^- \phi_n^- = \rho^+ \phi_0^+$ and $\frac{1}{h^-} (-\ell_0 \phi_n^- + \mathcal{L}_n^{(1)} \Phi^-) = \frac{1}{h^+} (\ell_0 \phi_0^+ + \mathcal{L}_0^{(1)} \Phi^+)$.

After some basic algebra, we obtain expressions of fields at the interface with respect to fields inside both layers:

$$\begin{aligned} \mathbf{w}_n^- &= \frac{1}{\ell_0 (h^- \rho^- + h^+ \rho^+)} \left[h^+ \begin{pmatrix} \rho^+ & 0 \\ 0 & \rho^+ \end{pmatrix} \mathcal{L}_n^{(2)} \mathbf{W}^- - h^- \begin{pmatrix} \rho^+ & 0 \\ 0 & \rho^- \end{pmatrix} \mathcal{L}_0^{(2)} \mathbf{W}^+ \right] \quad \text{and} \\ \mathbf{w}_0^+ &= \frac{1}{\ell_0 (h^- \rho^- + h^+ \rho^+)} \left[h^+ \begin{pmatrix} \rho^- & 0 \\ 0 & \rho^+ \end{pmatrix} \mathcal{L}_n^{(2)} \mathbf{W}^- - h^- \begin{pmatrix} \rho^- & 0 \\ 0 & \rho^- \end{pmatrix} \mathcal{L}_0^{(2)} \mathbf{W}^+ \right] . \end{aligned} \quad (\text{B.12})$$

Eq. (B.12) is directly of the form (11).

B.4.2 Viscoelastic solid/homogeneous fluid [Eq. (13), Table 2]

Continuity of vertical velocity and acoustic pressure at $z = z_I$ induces that: $v_z^-(z_I^-) = (\phi^+)'(z_I^+)$ and $\boldsymbol{\sigma}_z^-(z_I^-) = -\mathfrak{i} [k \mathcal{C}_{zx}^-(z_I^-) + \nu \mathcal{C}_{zy}^-(z_I^-)] \mathbf{u}^-(z_I^-) + \mathcal{C}_{zz}^-(z_I^-) (\mathbf{u}^-)'(z_I^-) = -p^+(z_I^+) \mathbf{n}$, where \mathbf{n} denotes the unit vector in the z -direction. As in Eq. (B.3), the matrices \mathcal{A}_n^- and \mathcal{B}_n^- are defined as follows:

$$\mathcal{A}_n^- = \mathcal{B}_n^- \left[\frac{1}{h^-} \mathcal{C}_{zz}(z_I^-) \right] \quad \text{with} \quad \mathcal{B}_n^- = \left\{ \frac{\ell_0}{h^-} \mathcal{C}_{zz}(z_I^-) + \mathfrak{i} [k \mathcal{C}_{zx}(z_I^-) + \nu \mathcal{C}_{zy}(z_I^-)] \right\}^{-1} . \quad (\text{B.13})$$

Thus, we obtain from Eq. (A.3) both the velocity in the z -direction and the displacement vector in the solid at the interface, with respect to the velocity potential and the acoustic pressure in the fluid at the interface and the displacement inside the solid. Their expressions are:

$$\mathbf{n} \cdot \mathbf{v}_n^- = \frac{1}{h^+} \left(\ell_0 \phi_0^+ + \mathcal{L}_0^{(1)} \Phi^+ \right) \quad \text{and} \quad \mathbf{u}_n^- = p_0^+ \mathcal{B}_n^- \mathbf{n} + \mathcal{A}_n^- \mathcal{L}_n^{(3)} \mathbf{U}^- , \quad (\text{B.14})$$

that give the following expression of the velocity vector in the solid at the interface:

$$\mathbf{v}_n^- = \mathbb{J} \mathcal{A}_n^- \mathcal{L}_n^{(3)} \mathbf{V}^- + \frac{1}{h^+} \left(\ell_0 \phi_0^+ + \mathcal{L}_0^{(1)} \Phi^+ \right) \mathbf{n} . \quad (\text{B.15})$$

Finally, after elimination of the displacement and velocity vectors in the solid at the interface, we obtain the eigenvalue-like equation on the local state vector \mathbf{w}_0^+ :

$$\mathfrak{i} \omega \mathbf{w}_0^+ = \mathfrak{i} \omega \mathbf{s}_I = \left\{ \begin{array}{c} -\frac{p_0^+}{\rho^+} \\ \frac{1}{\beta_n^-} \left[\frac{1}{h^+} \left(\ell_0 \phi_0^+ + \mathcal{L}_0^{(1)} \Phi^+ \right) - \mathbf{a}_n^- \cdot \mathbf{V}^- \right] \end{array} \right\} , \quad \text{with } \mathbf{s}_I = \begin{pmatrix} \phi_0^+ \\ p_0^+ \end{pmatrix} , \quad (\text{B.16})$$

where $\beta_n^- = \mathbf{n} \cdot (\mathcal{B}_n^- \mathbf{n})$ denotes the (3,3)-component of the matrix \mathcal{B}_n^- , and \mathbf{a}_n^- is the last row of the matrix $\mathcal{A}_n^- \mathcal{L}_n^{(3)}$. Consequently, in this particular case, a 2-dimensional **additional interfacial state vector** denoted \mathbf{s}_I must be introduced. With the definition (B.2) of the state vector in fluid, Eqs. (B.14) and (B.15) give the first equation of system (13). Eq. (B.16) provides the second equation of this system and the third, since $\mathbf{w}_0^+ = \mathbf{s}_I$. Of course, this last equation is strongly reduced.

B.4.3 Viscoelastic solid/viscoelastic solid [Eq. (11), Table 2]

The continuity of displacement, velocity and vertical-stress vectors gives:

$$\mathbf{w}_n^- = \mathbf{w}_0^+ = \begin{pmatrix} \mathcal{A}^+ & \mathbb{O}_3 \\ \mathbb{O}_3 & \mathcal{A}^+ \end{pmatrix} \mathcal{L}_0^{(6)} \mathbf{W}^+ - \begin{pmatrix} \mathcal{A}^- & \mathbb{O}_3 \\ \mathbb{O}_3 & \mathcal{A}^- \end{pmatrix} \mathcal{L}_n^{(6)} \mathbf{W}^- , \quad (\text{B.17})$$

where $\mathcal{B} = \{-\ell_0 [(1/h^+) \mathcal{C}_{zz}^+ + (1/h^-) \mathcal{C}_{zz}^-] + \mathfrak{i} [(k \mathcal{C}_{zx}^+ + \nu \mathcal{C}_{zy}^+) - (k \mathcal{C}_{zx}^- + \nu \mathcal{C}_{zy}^-)]\}^{-1}$, $\mathcal{A}^- = (1/h^-) \mathcal{B} \mathcal{C}_{zz}^-$ and $\mathcal{A}^+ = (1/h^+) \mathcal{B} \mathcal{C}_{zz}^+$. Eq. (B.17) gives the two state vectors to build the system (11).

C Detailed calculations for the *fixed-frequency problem*

C.1 Local state vector in homogeneous fluid [Eq. (8), Table 1]

The local state vector is two-dimensional. Its components are the displacement potential and the displacement in the x -direction. From Eqs.(3) and (4), the generic ODE (8) is expressed with the following vector and matrices:

$$\mathbf{w}(z) = \begin{bmatrix} \psi(z) \\ u_x(z) = -\mathfrak{i} k \psi(z) \end{bmatrix} , \quad M_0 = \begin{pmatrix} 0 & 1 \\ \nu^2 - \omega^2/c^2 & 0 \end{pmatrix} , \quad M_1 = \mathbb{O}_2 \quad \text{and} \quad M_2 = \begin{pmatrix} 0 & 0 \\ -1 & 0 \end{pmatrix} . \quad (\text{C.1})$$

C.2 Local state vector in viscoelastic solid [Eq. (8), Table 1]

In this case, where the angular frequency ω is considered as a parameter, the generalized Hooke's law (2) can be simply rewritten as follows:

$$\boldsymbol{\sigma}_\alpha(z) = -\mathfrak{i} [k \mathcal{C}_{\alpha x}(z, \omega) + \nu \mathcal{C}_{\alpha y}(z, \omega)] \mathbf{u}(z) + \mathcal{C}_{\alpha z}(z, \omega) \mathbf{u}'(z) , \quad \alpha = x, y, z . \quad (\text{C.2})$$

The generic ODE (8) is built with the following six-dimensional local state vector:

$$\mathbf{w}(z) = \begin{bmatrix} \mathbf{u}(z) \\ \mathbf{v}(z) = -\mathbf{i} k \mathbf{u}(z) \end{bmatrix}, \quad (\text{C.3})$$

remembering that the vector \mathbf{v} does not denote the velocity vector in the *fixed-frequency problem*.

From Eqs. (C.2) and (C.3), the matrices $M_2(z)$, $M_1(z)$ and $M_0(z)$ are the following 6-by-6 matrices:

$$M_2(z) = \begin{bmatrix} \mathbb{O}_3 & \mathbb{O}_3 \\ -\mathcal{C}_{xx}^{-1} \mathcal{C}_{zz} & \mathbb{O}_3 \end{bmatrix}, \quad M_1(z) = \left\{ \begin{array}{cc} \mathbb{O}_3 & \mathbb{O}_3 \\ \mathcal{C}_{xx}^{-1} [\mathbf{i} \nu (\mathcal{C}_{yz} + \mathcal{C}_{zy}) - \partial_z \mathcal{C}_{zz}] & -\mathcal{C}_{xx}^{-1} [(\mathcal{C}_{xz} + \mathcal{C}_{zx})] \end{array} \right\} \quad \text{and}$$

$$M_0(z) = \left\{ \begin{array}{cc} \mathbb{O}_3 & \mathbb{I}_3 \\ \mathcal{C}_{xx}^{-1} [\nu^2 \mathcal{C}_{yy} + \mathbf{i} \nu \partial_z \mathcal{C}_{zy} - \rho(z) \omega^2 \mathbb{I}_3] & \mathcal{C}_{xx}^{-1} [\mathbf{i} \nu (\mathcal{C}_{xy} + \mathcal{C}_{yx}) - \partial_z \mathcal{C}_{zx}] \end{array} \right\},$$

$\mathcal{C}_{\alpha\beta}(z, \omega)$ being simply denoted by $\mathcal{C}_{\alpha\beta}$.

C.3 External interface at $z = 0$

C.3.1 Rigid wall/homogeneous fluid [Eq. (17), Table 3]

The condition of zero normal displacement at $z = 0$ leads to: $\mathbf{w}'(0^+) = \mathbf{0}_2$. The approximation Eq. (A.3) directly gives the expression of the local state vector: $\mathbf{w}_u = -(\ell_0)^{-1} \mathcal{L}_0^{(2)} \mathbf{W}$.

C.3.2 Vacuum/homogeneous fluid [Eq. (17), Table 3]

The condition of zero acoustic pressure at $z = 0$ is: $\mathbf{w}(0^+) = \mathbf{w}_u = \mathbf{0}_2$.

C.3.3 Vacuum/viscoelastic solid [Eq. (17), Table 3]

Even though the results of this subsection concern only vacuum/viscoelastic solid external interfaces, the method used here will be useful to express stress, displacement and velocity fields in any solid independently of the external medium, *i.e.*, vacuum or fluid. A similar method is also used below to treat internal interfaces involving at least one solid layer.

By using Eq. (C.2) and the finite difference approximation Eq. (A.3) applied to $\mathbf{u}'(0^+)$, we obtain the following expression of the normal stress:

$$\boldsymbol{\sigma}_z(0^+) = C_{zx}^+ \mathbf{v}_0 + \mathcal{B}_u^{-1} \left[-\mathbf{u}_0 + \mathcal{A}_u \mathcal{L}_0^{(3)} \mathbf{U} \right], \quad (\text{C.4})$$

where $\mathbf{v}_0 = -\mathbf{i} k \mathbf{u}_0$ is not the velocity vector⁴, $\mathcal{B}_u = [(-\ell_0/h) \mathcal{C}_{zz}^+ + \mathbf{i} \nu \mathcal{C}_{zy}^+]^{-1}$ and $\mathcal{A}_u = h^{-1} \mathcal{B}_u \mathcal{C}_{zz}^+$. Note the similarity of this definition of the matrices \mathcal{A}_u and \mathcal{B}_u to Eq. (B.3) for the *fixed-wavenumber problem*. The zero normal stress condition immediately gives the expression of the displacement vector \mathbf{u}_0 at the interface such that:

$$\mathbf{u}_0 = \mathcal{B}_u \mathcal{C}_{zx}^+ \mathbf{v}_0 + \mathcal{A}_u \mathcal{L}_0^{(3)} \mathbf{U}, \quad (\text{C.5})$$

where the global vector \mathbf{U} contains the displacements at the inner nodes of the plate. Multiplying Eq. (C.5) by $(-\mathbf{i} k)$ gives: $(\mathcal{B}_u \mathcal{C}_{zx}^+) (-\mathbf{i} k \mathbf{v}_0) = \mathbf{v}_0 - \mathcal{A}_u \mathcal{L}_0^{(3)} \mathbf{V}$, where the \mathcal{C}_{zx}^+ matrix is generally not invertible.

For the elastic case and with the Voigt notation, this matrix takes the form: $\mathcal{C}_{zx} = \begin{pmatrix} C_{15} & C_{56} & C_{55} \\ C_{14} & C_{46} & C_{45} \\ C_{13} & C_{36} & C_{35} \end{pmatrix}$.

Remembering that the variations of propagation direction of guided waves are taken into account by rotating the crystallographic axes, this matrix can be full in many cases. Nevertheless, for both isotropic solids and

⁴In fact \mathbf{v}_0 denotes $\lambda \mathbf{u}_0$ which is the velocity vector only if $\lambda = \mathbf{i} \omega$, *i.e.*, for the other two *problems*.

wave propagation along one crystallographic axis of an orthorhombic medium, this matrix is not invertible and contains only two nonzero coefficients: $\mathcal{C}_{zx} = \begin{pmatrix} 0 & 0 & C_{55} \\ 0 & 0 & 0 \\ C_{13} & 0 & 0 \end{pmatrix}$.

Assuming that the matrix $\mathcal{B}_u \mathcal{C}_{zx}^+$ is diagonalizable leads to: $\mathcal{B}_u \mathcal{C}_{zx}^+ = \mathbf{X}_0 \text{diag}(\lambda_i) \mathbf{X}_0^{-1}$.

Considering the new vector \mathbf{r}_0 such that $\mathbf{v}_0 = \mathbf{X}_0 \mathbf{r}_0$ leads to: $-\mathfrak{i} k \text{diag}(\lambda_i) \mathbf{r}_0 = \mathbf{r}_0 - \mathbf{X}_0^{-1} \mathcal{A}_u \mathcal{L}_0^{(3)} \mathbf{V}$, where the eigenvalues λ_i are sorted by decreasing absolute values. The number of nonzero eigenvalues is the rank r of the matrix \mathcal{C}_{zx}^+ . To partially invert the latter equation, the three components of the vector \mathbf{r}_0 must be separated into two vectors \mathbf{r}_0^\perp and \mathbf{r}_0^{\parallel} of dimensions r and $3-r$, respectively. Doing so, we obtain:

$$-\mathfrak{i} k \mathbf{r}_0^\perp = \mathbf{\Lambda}_0^{-1} \left[\mathbf{r}_0^\perp - \mathbf{Y}_0^\perp \mathcal{A}_u \mathcal{L}_0^{(3)} \mathbf{V} \right], \quad \mathbf{r}_0^{\parallel} = \mathbf{Y}_0^{\parallel} \mathcal{A}_u \mathcal{L}_0^{(3)} \mathbf{V} \quad \text{and} \quad \mathbf{v}_0 = \mathbf{X}_0^\perp \mathbf{r}_0^\perp + \mathbf{X}_0^{\parallel} \mathbf{r}_0^{\parallel}, \quad (\text{C.6})$$

where $\mathbf{\Lambda}_0 = \text{diag}(\lambda_i)$ is an r -by- r diagonal invertible matrix. The r -by-3 matrix \mathbf{Y}_0^\perp and the $(3-r)$ -by-3 matrix \mathbf{Y}_0^{\parallel} are built by taking the first r rows and the last $(3-r)$ rows of the matrix \mathbf{X}_0^{-1} , respectively. Similarly, \mathbf{X}_0^\perp and \mathbf{X}_0^{\parallel} denote the matrices built by taking the first r columns and the last $(3-r)$ columns of the matrix \mathbf{X}_0 , respectively. Finally, by replacing the vector \mathbf{r}_0^{\parallel} in the expression of \mathbf{v}_0 and rewriting Eq. (C.5) with Eq. (C.6), the subvectors \mathbf{u}_0 and \mathbf{v}_0 of the local state vector \mathbf{w}_u at the interface with respect to the state vectors $\mathbf{r}_0^\perp = \mathbf{Y}_0^\perp \mathbf{v}_0$, \mathbf{U} and \mathbf{V} are expressed as follows:

$$\mathbf{u}_0 = \mathbf{X}_0^\perp \mathbf{\Lambda}_0 \mathbf{r}_0^\perp + \mathcal{A}_u \mathcal{L}_0^{(3)} \mathbf{U} \quad \text{and} \quad \mathbf{v}_0 = \mathbf{X}_0^\perp \mathbf{r}_0^\perp + \mathbf{X}_0^{\parallel} \mathbf{Y}_0^{\parallel} \mathcal{A}_u \mathcal{L}_0^{(3)} \mathbf{V}. \quad (\text{C.7})$$

Introducing the **interfacial state vector** $\mathbf{s}_u = \mathbf{r}_0^\perp$ and with the first equation of (C.6), the identification of Eq. (17) is then immediate.

C.3.4 Homogeneous fluid/homogeneous fluid [Eq. (21), Table 3]

From the wave definition in half-spaces given in Eq. (6), continuity of both vertical displacement and acoustic pressure at $z = 0$ yields: $\mathfrak{i} \kappa_u(k, \omega) \psi_u = \psi'(0^+)$ and $p_u = p(0^+)$, which implies: $\rho_u \psi_u = \rho \psi(0^+)$. By using the expression given in §C.1, the local state vector \mathbf{w}_u of the plate at $z = 0$ is deduced as follows:

$$\mathbf{w}_u = \begin{bmatrix} \psi(0^+) \\ -\mathfrak{i} k \psi(0^+) \end{bmatrix} = \frac{\rho_u}{\rho} \begin{pmatrix} \psi_u \\ u_{ux} \end{pmatrix} = \frac{\rho_u}{\rho} \mathbf{w}(0^-) = \frac{\rho_u}{\rho} \mathbf{s}_u, \quad (\text{C.8})$$

where the **interfacial state vector** \mathbf{s}_u has been introduced and coincides with the local state vector $\mathbf{w}(0^-)$ in the external fluid. Calculating the derivative $\mathbf{w}'(0^-)$ by using approximation Eq. (A.3) gives:

$$\mathfrak{i} \kappa_u(k, \omega) \mathbf{w}_u = \frac{\rho_u}{\rho} [\mathfrak{i} \kappa_u(k, \omega) \mathbf{s}_u] = \frac{\rho_u}{\rho} \left[\frac{\rho_u \ell_0}{\rho h} \mathbf{s}_u + \frac{1}{h} \mathcal{L}_0^{(2)} \mathbf{W} \right]. \quad (\text{C.9})$$

The state variables in the external fluid satisfy the eigenvalue-like equations:

$$\begin{aligned} -\mathfrak{i} k \psi_u &= u_{ux} \quad \text{and} \\ -\mathfrak{i} k u_{ux} &= -\frac{\rho_u \ell_0}{\rho h^2} \mathcal{L}_0^{(1)} \mathbf{\Psi} - \frac{1}{h} \mathcal{L}_0^{(1)} [\mathfrak{i} \kappa_u(k, \omega) \mathbf{\Psi}] + \left[\nu^2 - \frac{\omega^2}{c_u^2} - \left(\frac{\rho_u \ell_0}{\rho h} \right)^2 \right] \psi_u. \end{aligned} \quad (\text{C.10})$$

From Eqs. (C.10), (C.8) and (C.9), Eqs. (21.a), (21.b) and (21.c) can be identified, respectively.

⁵ $r = 2$ in most cases.

C.3.5 Homogeneous fluid/viscoelastic solid [Eq. (21), Table 3]

Using the notation introduced for the vacuum/solid case, the normal stress at the interface in the solid is given by Eq. (C.4). When writing the continuity of vertical stress vector, the presence of fluid instead of vacuum induces changes in Eqs. (C.6) and (C.7). The subvectors \mathbf{u}_0 and \mathbf{v}_0 of the local state vector \mathbf{w}_u and the interfacial vector \mathbf{r}_0^\perp now satisfy the following equations:

$$\begin{aligned}\mathbf{u}_0 &= \mathbf{X}_0^\perp \boldsymbol{\Lambda}_0 \mathbf{r}_0^\perp + \mathcal{A}_u \mathcal{L}_0^{(3)} \mathbf{U} + \rho_u \omega^2 \psi_u \mathbf{b}_u, \\ \mathbf{v}_0 &= \mathbf{X}_0^\perp \mathbf{r}_0^\perp + \mathbf{X}_0'' \mathbf{Y}_0'' \left(\mathcal{A}_u \mathcal{L}_0^{(3)} \mathbf{V} + \rho_u \omega^2 u_{ux} \mathbf{b}_u \right) \text{ and} \\ -\mathfrak{i} k \mathbf{r}_0^\perp &= \boldsymbol{\Lambda}_0^{-1} \left[\mathbf{r}_0^\perp - \mathbf{Y}_0^\perp \left(\mathcal{A}_u \mathcal{L}_0^{(3)} \mathbf{V} + \rho_u \omega^2 u_{ux} \mathbf{b}_u \right) \right],\end{aligned}\tag{C.11}$$

where the new vector \mathbf{b}_u is the last column of the matrix \mathcal{B}_u defined in Eq. (C.4). Note that u_{ux} denotes the displacement in the x -direction in the fluid and, of course, is different from the first component of the displacement vector \mathbf{u}_0 in the solid. The variable ψ_u stands for the displacement potential in the fluid. In regard to the vacuum/solid case, the vector \mathbf{r}_0^\perp must be appended to the interfacial state vector \mathbf{s}_u because it satisfies the eigenvalue-like equation being the last row of Eq. (C.11). The continuity of the vertical displacement immediately gives: $\mathfrak{i} \kappa_u(k, \omega) \psi_u = \mathbf{n} \cdot \mathbf{u}_0$ and $\mathfrak{i} \kappa_u(k, \omega) u_{ux} = \mathbf{n} \cdot \mathbf{v}_0$, which leads with Eq. (C.11) to the following expressions of $\mathfrak{i} \kappa_u(k, \omega) \mathbf{u}_0$ and $\mathfrak{i} \kappa_u(k, \omega) \mathbf{v}_0$:

$$\begin{aligned}\mathfrak{i} \kappa_u(k, \omega) \mathbf{u}_0 &= \mathbf{X}_0^\perp \boldsymbol{\Lambda}_0 \left[\mathfrak{i} \kappa_u(k, \omega) \mathbf{r}_0^\perp \right] + \mathcal{A}_u \mathcal{L}_0^{(3)} \left[\mathfrak{i} \kappa_u(k, \omega) \mathbf{U} \right] + \rho_u \omega^2 (\mathbf{n} \cdot \mathbf{u}_0) \mathbf{b}_u \text{ and} \\ \mathfrak{i} \kappa_u(k, \omega) \mathbf{v}_0 &= \mathbf{X}_0^\perp \left[\mathfrak{i} \kappa_u(k, \omega) \mathbf{r}_0^\perp \right] + \mathbf{X}_0'' \mathbf{Y}_0'' \left(\mathcal{A}_u \mathcal{L}_0^{(3)} \left[\mathfrak{i} \kappa_u(k, \omega) \mathbf{V} \right] + \rho_u \omega^2 (\mathbf{n} \cdot \mathbf{v}_0) \mathbf{b}_u \right),\end{aligned}\tag{C.12}$$

where the vectors \mathbf{u}_0 and \mathbf{v}_0 will be easily replaced in $(\mathbf{n} \cdot \mathbf{u}_0)$ and $(\mathbf{n} \cdot \mathbf{v}_0)$ by the expressions given in Eq. (C.11). Thus, from Eq. (C.1), we need to express the eigenvalue-like equations linking the two components of the interfacial state vector in the fluid as follows:

$$\begin{aligned}-\mathfrak{i} k \psi_u &= u_{ux} \text{ and} \\ -\mathfrak{i} k u_{ux} &= -k^2 \psi_u = \left(\kappa_u^2(k, \omega) + \nu^2 - \frac{\omega^2}{c_u^2} \right) \psi_u = -\mathbf{n} \cdot \left[\mathfrak{i} \kappa_u(k, \omega) \mathbf{u}_0 \right] + \left(\nu^2 - \frac{\omega^2}{c_u^2} \right) \psi_u.\end{aligned}\tag{C.13}$$

Last, the state vector $\left[\mathfrak{i} \kappa_u(k, \omega) \mathbf{r}_0^\perp \right]$ that must be appended to complete the interfacial state vector \mathbf{s}_u satisfies the following eigenvalue-like equation:

$$-\mathfrak{i} k \left[\mathfrak{i} \kappa_u(k, \omega) \mathbf{r}_0^\perp \right] = \boldsymbol{\Lambda}_0^{-1} \left\{ \left[\mathfrak{i} \kappa_u(k, \omega) \mathbf{r}_0^\perp \right] - \mathbf{Y}_0^\perp \mathcal{A}_u \mathcal{L}_0^{(3)} \left[\mathfrak{i} \kappa_u(k, \omega) \mathbf{V} \right] - \rho_u \omega^2 (\mathbf{n} \cdot \mathbf{v}_0) \mathbf{Y}_0^\perp \mathbf{b}_u \right\}.\tag{C.14}$$

Finally, from Eqs. (C.11) to (C.14), all the elements to obtain the matrices defined in System (21) can be identified.

C.4 Internal interfaces

C.4.1 Homogeneous fluid/homogeneous fluid [Eq. (11), Table 2]

The equations of continuity of both vertical displacement and acoustic pressure at the interface immediately give:

$$\mathbf{w}_n^- = \rho^+ \mathbf{w}_I \text{ and } \mathbf{w}_0^+ = \rho^- \mathbf{w}_I, \text{ where } \mathbf{w}_I = \frac{1}{\ell_0 (\rho^- h^- + \rho^+ h^+)} \left[h^+ \mathcal{L}_n^{(2)} \mathbf{W}^- - h^- \mathcal{L}_0^{(2)} \mathbf{W}^+ \right].\tag{C.15}$$

These two equations lead immediately to Eq. (11).

C.4.2 Homogeneous fluid/viscoelastic solid [Eq. (13), Table 2]

The continuity of the vertical displacement yields:

$$\frac{1}{h^-} [-\ell_0 \psi_n^- + \mathcal{L}_n^{(1)} \Psi^-] = \mathbf{n} \cdot \mathbf{u}_0^+ \quad \text{and} \quad \frac{1}{h^-} [-\ell_0 u_{nx}^- + \mathcal{L}_n^{(1)} \mathbf{U}_x^-] = \mathbf{n} \cdot \mathbf{v}_0^+ . \quad (\text{C.16})$$

The combination of Eq. (C.16) and Eq. (C.11), the latter expressing the continuity of the vertical stress vector at the interface, gives the expressions of the displacement potential ψ_n^- and the displacement u_{nx}^- in the fluid at the interface, *i.e.*, the components of the local state vector \mathbf{w}_n^- , such that

$$\begin{aligned} \psi_n^- &= \frac{1}{\ell_0 + \omega^2 \rho^- h^- \mathbf{n} \cdot \mathbf{b}_0} \left[\mathcal{L}_n^{(1)} \Psi^- - h^- \mathbf{n} \cdot \left(\mathbf{X}_0^\perp \boldsymbol{\Lambda}_0 \mathbf{r}_0^\perp + \mathcal{A}_u \mathcal{L}_0^{(3)} \mathbf{U}^+ \right) \right] \quad \text{and} \\ u_{nx}^- &= \frac{1}{\ell_0 + \omega^2 \rho^- h^- \mathbf{n} \cdot (\mathbf{X}_0^\parallel \mathbf{Y}_0^\parallel \mathbf{b}_0)} \left[\mathcal{L}_n^{(1)} \mathbf{U}_x^- - h^- \mathbf{n} \cdot \left(\mathbf{X}_0^\perp \mathbf{r}_0^\perp + \mathbf{X}_0^\parallel \mathbf{Y}_0^\parallel \mathcal{A}_u \mathcal{L}_0^{(3)} \mathbf{V}^+ \right) \right] . \end{aligned} \quad (\text{C.17})$$

On rewriting Eq. (C.11) with the notations of this section, the following expressions:

$$\begin{aligned} \mathbf{u}_0^+ &= \mathbf{X}_0^\perp \boldsymbol{\Lambda}_0 \mathbf{r}_0^\perp + \mathcal{A}_u \mathcal{L}_0^{(3)} \mathbf{U}^+ + \omega^2 \rho^- \psi_n^- \mathbf{b}_u \\ \mathbf{v}_0^+ &= \mathbf{X}_0^\perp \mathbf{r}_0^\perp + \mathbf{X}_0^\parallel \mathbf{Y}_0^\parallel \left(\mathcal{A}_u \mathcal{L}_0^{(3)} \mathbf{V}^+ + \omega^2 \rho^- u_{nx}^- \mathbf{b}_u \right) \\ -i k \mathbf{r}_0^\perp &= \boldsymbol{\Lambda}_0^{-1} \left[\mathbf{r}_0^\perp - \mathbf{Y}_0^\perp \left(\mathcal{A}_u \mathcal{L}_0^{(3)} \mathbf{V}^+ + \omega^2 \rho^- u_{nx}^- \mathbf{b}_u \right) \right] \end{aligned} \quad (\text{C.18})$$

give the two components \mathbf{u}_0^+ and \mathbf{v}_0^+ of the local state vector \mathbf{w}_0^+ in the solid and the eigenvalue-like equation with respect to the **additional interfacial state vector** $\mathbf{s}_I = \mathbf{r}_0^\perp$. Consequently, with the state vector definitions given in § C.1 and § C.2, the above equations (C.17) and (C.18) provide system (13).

C.4.3 Viscoelastic solid/viscoelastic solid [Eq. (13), Table 2]

The continuity of displacements $\mathbf{u}_n^- = \mathbf{u}_0^+$ implies $\mathbf{v}_n^- = \mathbf{v}_0^+$. As a consequence, the two local state vectors in both solids, defined by Eq. C.3, are such that:

$$\mathbf{w}_n^- = \mathbf{w}_0^+ . \quad (\text{C.19})$$

Thus, only one of these two vectors has to be expressed. Let us choose the vector \mathbf{w}_n^- . The continuity of normal stress leads to:

$$\mathbf{u}_n^- = \mathcal{M} \mathbf{v}_n^- + \mathcal{A}^+ \mathcal{L}_0^{(3)} \mathbf{U}^+ - \mathcal{A}^- \mathcal{L}_n^{(3)} \mathbf{U}^- , \quad (\text{C.20})$$

where $\mathcal{A}^- = (1/h^-) \mathcal{B} \mathcal{C}_{zz}^-$, $\mathcal{A}^+ = (1/h^+) \mathcal{B} \mathcal{C}_{zz}^+$ and $\mathcal{M} = \mathcal{B} (\mathcal{C}_{zx}^+ - \mathcal{C}_{zx}^-)$,

with $\mathcal{B} = \{-\ell_0 [(1/h^+) \mathcal{C}_{zz}^+ + (1/h^-) \mathcal{C}_{zz}^-] + i \nu (\mathcal{C}_{zy}^+ - \mathcal{C}_{zy}^-)\}^{-1}$.

In the same way as Eqs. (C.6) and (C.7) have been obtained above from Eq. (C.5) for the solid/vacuum case, here, Eq. (C.20) leads to the following equations, with suitable notations:

$$\begin{aligned} \mathbf{u}_n^- &= \mathbf{X}^\perp \boldsymbol{\Lambda} \mathbf{r}^\perp + \left(\mathcal{A}^+ \mathcal{L}_0^{(3)} \mathbf{U}^+ - \mathcal{A}^- \mathcal{L}_n^{(3)} \mathbf{U}^- \right) , \\ \mathbf{v}_n^- &= \mathbf{X}^\perp \mathbf{r}^\perp + \mathbf{X}^\parallel \mathbf{Y}^\parallel \left(\mathcal{A}^+ \mathcal{L}_0^{(3)} \mathbf{V}^+ - \mathcal{A}^- \mathcal{L}_n^{(3)} \mathbf{V}^- \right) \quad \text{and} \\ -i k \mathbf{r}^\perp &= \boldsymbol{\Lambda}^{-1} \left[\mathbf{r}^\perp - \mathbf{Y}^\perp \left(\mathcal{A}^+ \mathcal{L}_0^{(3)} \mathbf{V}^+ - \mathcal{A}^- \mathcal{L}_n^{(3)} \mathbf{V}^- \right) \right] . \end{aligned} \quad (\text{C.21})$$

An **interfacial state vector** $\mathbf{s}_I = \mathbf{r}^\perp$ of dimension the rank r of the \mathcal{M} matrix has been introduced. Finally, with Eqs. (C.19) and (C.21), the system (13) can be identified. To conclude, note that if $\mathcal{C}_{zx}^- = \mathcal{C}_{zx}^+$, there is no interfacial state vector, *i.e.*, its rank is zero, and Eq. (C.21) simply becomes: $\mathbf{u}_n^- = \mathcal{A}^+ \mathcal{L}_0^{(3)} \mathbf{U}^+ - \mathcal{A}^- \mathcal{L}_n^{(3)} \mathbf{U}^-$ and $\mathbf{v}_n^- = \mathcal{A}^+ \mathcal{L}_0^{(3)} \mathbf{V}^+ - \mathcal{A}^- \mathcal{L}_n^{(3)} \mathbf{V}^-$. These two equations are the same as for the *fixed-wavenumber problem* [*cf.* Eq. (B.17)].

D Detailed calculations for the *fixed-slowness problem*

For this problem, the horizontal slowness vector is fixed and the frequency ω becomes the variable to be found. The slowness horizontal vector can be arbitrarily directed along the x -axis. Consequently, if s denotes the slowness in the x -direction, the two vertical slownesses τ_u and τ_ℓ , in the upper and lower external fluids, respectively, are such that:

$$\tau_u = \pm \sqrt{\frac{1}{c_u^2} - s^2} \quad \text{and} \quad \tau_\ell = \pm \sqrt{\frac{1}{c_\ell^2} - s^2}, \quad (\text{D.1})$$

where, by using Eq. (5): $k = \omega s$, $\nu = 0$, $\kappa_u = \omega \tau_u$ and $\kappa_\ell = \omega \tau_\ell$.

The issues of this third case are quite different from the others; therefore, they are further away from the main topic of the present paper. Consequently, we consider here only the simple case of homogeneous fluids and homogeneous elastic solids.

D.1 Local state vector in homogeneous fluid [Eq. (8), Table 1]

Let us consider the acoustic pressure $p(z)$ and the velocity potential $\phi(z)$. From Eqs. (3) and (4), these two fields are linked by the following equations:

$$\mathfrak{i} \omega \phi(z) = -\frac{1}{\rho} p(z) \quad \text{and} \quad \mathfrak{i} \omega \left(s^2 - \frac{1}{c^2} \right) p(z) = \rho \phi''(z). \quad (\text{D.2})$$

There is a degenerate case when $s = 1/c$. This means that a plane wave propagates in the x -direction such that the vertical velocity $v_z(z) = \phi'(z) = v_0$ is uniform on the layer and $p(z) = \mathfrak{i} \omega \rho v_0 z + p(0)$. In this case, the global state vector of the layer is reduced to a single value v_0 such that $\mathfrak{i} \omega v_0 = (p(\ell) - p(0))/(\rho \ell)$.

In the other cases, *i.e.*, under subsonic or supersonic conditions, the two-dimensional local state vector $\mathbf{w}(z)$ and the matrices M_0 , M_1 and M_2 in the generic ODE (8) are such that:

$$\mathbf{w}(z) = \begin{bmatrix} \phi(z) \\ p(z) \end{bmatrix}, \quad M_0 = \begin{bmatrix} 0 & -1/\rho \\ 0 & 0 \end{bmatrix}, \quad M_1 = \mathbb{O}_2 \quad \text{and} \quad M_2 = \begin{bmatrix} 0 & 0 \\ -\alpha(s) & 0 \end{bmatrix}, \quad \text{where} \quad \alpha(s) = \frac{\rho c^2}{1 - s^2 c^2} = \frac{\rho}{\tau(s)^2}. \quad (\text{D.3})$$

D.2 Local state vector in homogeneous Elastic solid [Eq. (8), Table 1]

Newton's second law (1) and the standard Hooke's law (2) for a homogeneous elastic solid lead to:

$$\mathfrak{i} \omega (s^2 \mathcal{C}_{xx} - \rho \mathbb{I}_3) \mathbf{v}(z) = s (\mathcal{C}_{xz} + \mathcal{C}_{zx}) \mathbf{v}'(z) - \mathcal{C}_{zz} \mathbf{u}''(z). \quad (\text{D.4})$$

The stiffness matrix \mathcal{C}_{xx} is symmetric positive definite. Basically, it admits three eigenvalues ρc_i^2 ($i \in \{1, 2, 3\}$) and an orthogonal polarization matrix \mathcal{P} such that $\mathcal{C}_{xx} = \rho \mathcal{P} \text{diag}(c_i^2) \mathcal{P}^T$. In the isotropic

case, $c_1 = c_L$ and $c_2 = c_3 = c_T$ are the longitudinal and transverse sound speeds, respectively. Thus, Eq. (D.4) becomes:

$$\mathfrak{i} \omega \text{diag}_{i \in \{1, 2, 3\}} (s^2 c_i^2 - 1) \mathcal{P}^T \mathbf{v}(z) = \frac{1}{\rho} \mathcal{P}^T [s (\mathcal{C}_{xz} + \mathcal{C}_{zx}) \mathbf{v}'(z) - \mathcal{C}_{zz} \mathbf{u}''(z)]. \quad (\text{D.5})$$

Consequently, similar to fluids, degenerate cases occur when $s = 1/c_i$, *i.e.*, the slowness corresponds to a bulk wave propagating in the x -direction. This situation is not detailed here. For nondegenerate cases, the generic ODE (8) is satisfied for the following six-dimensional local state vector $\mathbf{w}(z)$ and matrices:

$$\mathbf{w}(z) = \begin{bmatrix} \mathbf{u}(z) \\ \mathbf{v}(z) = \mathfrak{i} \omega \mathbf{u}(z) \end{bmatrix}, \quad M_0 = \begin{bmatrix} \mathbb{O}_3 & \mathbb{I}_3 \\ \mathbb{O}_3 & \mathbb{O}_3 \end{bmatrix}, \quad (\text{D.6})$$

$$M_1 = \begin{bmatrix} \mathbb{O}_3 & \mathbb{O}_3 \\ \mathbb{O}_3 & s (s^2 \mathcal{C}_{xx} - \rho \mathbb{I}_3)^{-1} (\mathcal{C}_{xz} + \mathcal{C}_{zx}) \end{bmatrix} \quad \text{and} \quad M_2 = \begin{bmatrix} \mathbb{O}_3 & \mathbb{O}_3 \\ - (s^2 \mathcal{C}_{xx} - \rho \mathbb{I}_3)^{-1} \mathcal{C}_{zz} & \mathbb{O}_3 \end{bmatrix}.$$

D.3 External interface at $z = 0$

D.3.1 Rigid wall/homogeneous fluid [Eq. (17), Table 3]

For rigid walls, the boundary condition is such that the normal displacement is zero, *i.e.*, $\mathbf{w}'(0^+) = \mathbf{0}_2$. By using approximation Eq. (A.3), the state vector \mathbf{w}_u at the interface is immediately expressed with respect to the global state vector \mathbf{W} by: $\mathbf{w}_u = -(\ell_0)^{-1} \mathcal{L}_0^{(2)} \mathbf{W}$.

D.3.2 Vacuum/homogeneous fluid [Eq. (17), Table 3]

At a vacuum interface, both acoustic pressure and potentials are zero, *i.e.*, $\mathbf{w}(0^+) = \mathbf{w}_u = \mathbf{0}_2$.

D.3.3 Vacuum/homogeneous elastic solid [Eq. (17), Table 3]

Writing that the vertical stress vector $\boldsymbol{\sigma}_z(0^+)$ in the solid is zero at the interface $z = 0$ leads to: $i\omega s \mathcal{C}_{zx} \mathbf{u}_0 = s \mathcal{C}_{zx} \mathbf{v}_0 = \frac{1}{h} \mathcal{C}_{zz} \left(\ell_0 \mathbf{u}_0 + \mathcal{L}_0^{(3)} \mathbf{U} \right)$ and $i\omega s \mathcal{C}_{zx} \mathbf{v}_0 = \frac{1}{h} \mathcal{C}_{zz} \left(\ell_0 \mathbf{v}_0 + \mathcal{L}_0^{(3)} \mathbf{V} \right)$.

As in § C.3, Eq. (C.6), after the diagonalization of the matrix $\mathcal{B}_u \mathcal{C}_{zx}$, where $\mathcal{B}_u = (-h/\ell_0) \mathcal{C}_{zz}^{-1}$, we obtain the following equations:

$$\mathbf{u}_0 = -s \mathbf{X}_0^\perp \boldsymbol{\Lambda} \mathbf{r}_0^\perp - \frac{1}{\ell_0} \mathcal{L}_0^{(3)} \mathbf{U}, \quad \mathbf{v}_0 = \mathbf{X}_0^\perp \mathbf{r}_0^\perp - \frac{1}{\ell_0} \mathbf{X}_0^{\parallel} \mathbf{Y}_0^{\parallel} \mathcal{L}_0^{(3)} \mathbf{V} \quad \text{and} \quad i\omega \mathbf{r}_0^\perp = -\frac{1}{s} \boldsymbol{\Lambda}^{-1} \left[\mathbf{r}_0^\perp + \frac{1}{\ell_0} \mathbf{Y}_0^\perp \mathcal{L}_0^{(3)} \mathbf{V} \right]. \quad (\text{D.7})$$

Let the **vector \mathbf{r}_0^\perp** be the **interfacial state vector \mathbf{s}_u** . As a result, with the local state vector given in Eq. (D.6), system (17) is obtained.

D.3.4 Homogeneous fluid/homogeneous fluid [Eq. (17), Table 3]

Analogous to the previous cases, we consider only the nondegenerate case where the slowness s is assumed to be different from $1/c$. The continuity of acoustic pressure at the interface with Eq. (D.2) directly implies that the local state vector \mathbf{w}_u at the interface in the first fluid layer satisfies:

$$\mathbf{w}_u = \mathbf{w}(0^+) = \begin{bmatrix} \phi(0^+) \\ p(0^+) \end{bmatrix} = \begin{pmatrix} \rho_u/\rho & 0 \\ 0 & 1 \end{pmatrix} \begin{pmatrix} \phi_u \\ p_u \end{pmatrix}, \quad (\text{D.8})$$

where ϕ_u and p_u are the two components of the local state vector at the interface in the external fluid. Due to the definition (D.1) of the vertical slowness τ_u , approximation Eq. (A.3) and Eq. (D.2), the continuity of vertical displacement yields:

$$v_{z0} = -\frac{\tau_u}{\rho_u} p_u = \frac{1}{h} \left[\ell_0 \phi(0^+) + \mathcal{L}_0^{(1)} \boldsymbol{\Phi} \right] = \frac{1}{h} \left[\frac{\ell_0 \rho_u}{\rho} \phi_u + \mathcal{L}_0^{(1)} \boldsymbol{\Phi} \right]. \quad (\text{D.9})$$

From Eqs. (D.2) and (D.9), both the following expression of the acoustic pressure p_u at the interface and the following eigenvalue-like equation with respect to ϕ_u are obtained:

$$p_u = -\frac{\rho_u}{\tau_u h} \left[\frac{\ell_0 \rho_u}{\rho} \phi_u + \mathcal{L}_0^{(1)} \boldsymbol{\Phi} \right] \quad \text{and} \quad i\omega \phi_u = \frac{1}{\tau_u h} \left[\frac{\ell_0 \rho_u}{\rho} \phi_u + \mathcal{L}_0^{(1)} \boldsymbol{\Phi} \right]. \quad (\text{D.10})$$

Setting the **interfacial state vector \mathbf{s}_u** as the one-dimensional vector consisting of the velocity potential ϕ_u , Eq. (17) can be written without difficulty.

D.3.5 Homogeneous fluid/homogeneous elastic solid [Eq. (17), Table 3]

This case is similar to the vacuum/solid interface, keeping the same equations (D.7). The only difference is that the \mathcal{C}_{zx} matrix is replaced by $\{\mathcal{C}_{zx} + [\rho_u/(s\tau_u)] \mathbf{n} \otimes \mathbf{n}\}$, assuming that the vertical slowness τ_u is nonzero, *i.e.*, the case is not degenerate. It comes from the continuity of the vertical stress vector and Eq. (D.9):

$$-p_u \mathbf{n} = \frac{\rho_u}{\tau_u} (\mathbf{n} \cdot \mathbf{v}_0) \mathbf{n} = \frac{\rho_u}{\tau_u} (\mathbf{n} \otimes \mathbf{n}) \mathbf{v}_0 = -s \mathcal{C}_{zx} \mathbf{v}_0 + \frac{1}{h} \mathcal{C}_{zz} \left(\ell_0 \mathbf{u}_0 + \mathcal{L}_0^{(3)} \mathbf{U} \right).$$

D.4 Internal interfaces

D.4.1 Homogeneous fluid/homogeneous fluid [Eq. (11), Table 2]

For nondegenerate cases, *i.e.*, $s \neq 1/c^-$ and $s \neq 1/c^+$, because the local state vector is the same as that for the *fixed-wavenumber problem*, the state vectors \mathbf{w}_n^- and \mathbf{w}_0^+ at the interface are given by Eq. (B.12).

D.4.2 Homogeneous fluid/homogeneous elastic solid [Eq. (13), Table 2]

This case is the most difficult to handle. The two displacement and velocity vectors in the solid at the interface have to be separated into two in-plane vectors \mathbf{u}_0^+ and \mathbf{v}_0^+ and two vertical components u_z and v_z , such that:

$$\mathbf{u}_0^+ = \mathbb{P}^T \mathbf{u}_0^{[xy]} + u_z \mathbf{n} \quad \text{and} \quad \mathbf{v}_0^+ = \mathbb{P}^T \mathbf{v}_0^{[xy]} + v_z \mathbf{n}, \quad \text{where } \mathbb{P} = \begin{pmatrix} 1 & 0 & 0 \\ 0 & 1 & 0 \end{pmatrix}. \quad (\text{D.11})$$

The continuity of vertical velocity gives the following eigenvalue-like equation:

$$i\omega u_z = v_z = \frac{1}{h^-} \left(-\ell_0 \phi_n^- + \mathcal{L}_n^{(1)} \Phi^- \right). \quad (\text{D.12})$$

The continuity of the vertical stress vector gives:

$$\mathbf{0} = -s \mathbb{P} \mathcal{C}_{zx}^+ \mathbf{v}_0^+ + \frac{1}{h^+} \mathbb{P} \mathcal{C}_{zz}^+ \left(\ell_0 \mathbf{u}_0^+ + \mathcal{L}_0^{(3)} \mathbf{U}^+ \right) \quad \text{and} \quad p_n^- = -\mathbf{n} \cdot \left[-s \mathcal{C}_{zx}^+ \mathbf{v}_0^+ + \frac{1}{h^+} \mathcal{C}_{zz}^+ \left(\ell_0 \mathbf{u}_0^+ + \mathcal{L}_0^{(3)} \mathbf{U}^+ \right) \right]. \quad (\text{D.13})$$

To separate the displacement field into the horizontal and vertical contributions, let us consider the 2D vectors $\mathbf{c}_{\lambda\mu}^{[xy]} = \mathbb{P} \mathcal{C}_{\lambda\mu}^+ \mathbf{n}$ and the 2-by-2 matrices $\mathcal{C}_{\lambda\mu}^{[xy]} = \mathbb{P} \mathcal{C}_{\lambda\mu}^+ \mathbb{P}^T$. Then, Eqs. (D.11) and (D.13) give the following 2D linear system characterizing the zero normal shear stress condition at the interface:

$$s \left(\mathcal{C}_{zx}^{[xy]} \mathbf{v}_0^{[xy]} + v_z \mathbf{c}_{zx}^{[xy]} \right) = \frac{1}{h^+} \left[\ell_0 \left(\mathcal{C}_{zz}^{[xy]} \mathbf{u}_0^{[xy]} + u_z \mathbf{c}_{zz}^{[xy]} \right) + \mathbb{P} \mathcal{C}_{zz}^+ \mathcal{L}_0^{(3)} \mathbf{U}^+ \right]. \quad (\text{D.14})$$

Following a technique analogous to the one used for the vacuum/solid viscoelastic solid interface in section C.3.3, the matrix $\mathcal{B}_{xy} = (-h^+/\ell_0) (\mathcal{C}_{zz}^{[xy]})^{-1}$ is introduced. Then, the matrix $\mathcal{M}_{xy} = \mathcal{B}_{xy} \mathcal{C}_{zx}^{[xy]}$ of rank r is diagonalized such that $\mathcal{M}_{xy} = \mathbf{X}_{xy}^\perp \mathbf{\Lambda}_{xy} \mathbf{Y}_{xy}^\perp$. Finally, on defining a r -dimensional state vector \mathbf{r}_{xy}^\perp such that $\mathbf{r}_{xy}^\perp = \mathbf{Y}_{xy}^\perp \mathbf{v}_0^{[xy]}$, the horizontal displacement is expressed by:

$$\mathbf{u}_0^{[xy]} = -s \mathbf{X}_{xy}^\perp \mathbf{\Lambda}_{xy} \mathbf{r}_{xy}^\perp + \mathbf{u}_{xy}, \quad (\text{D.15})$$

where $\mathbf{u}_{xy} = \mathcal{B}_{xy} \left[-\frac{s}{h^-} (-\ell_0 \phi_n^- + \mathcal{L}_n^{(1)} \Phi^-) \mathbf{c}_{zx}^{[xy]} + \frac{1}{h^+} \left(\ell_0 u_z \mathbf{c}_{zz}^{[xy]} + \mathbb{P} \mathcal{C}_{zz}^+ \mathcal{L}_0^{(3)} \mathbf{U}^+ \right) \right]$. Let us note that if the rank r is zero, *e.g.*, for orthorhombic crystals, Eq. (D.15) simply reduces to $\mathbf{u}_0^{[xy]} = \mathbf{u}_{xy}$.

The **interfacial state vector** \mathbf{s}_I contains the **velocity potential** ϕ_n^- in the fluid, the **vertical displacement** u_z and the **in-plane vector** \mathbf{r}_{xy}^\perp of dimension in $\{0, 1, 2\}$. By using the state equation in the fluid, see Eq. (4), Eq. (D.12), and the product by $i\omega$ of Eq. (D.15), we obtain the following equations:

$$i\omega \phi_n^- = \frac{-1}{\rho^-} p_n^-, \quad i\omega \mathbf{r}_{xy}^\perp = \frac{-1}{s} \mathbf{\Lambda}_{xy}^{-1} \left[\mathbf{r}_{xy}^\perp - \mathbf{Y}_{xy}^\perp \mathbf{v}_{xy} \right] \quad \text{and} \quad \mathbf{v}_0^{[xy]} = \mathbf{X}_{xy}^\perp \mathbf{r}_{xy}^\perp + \mathbf{X}_{xy}^{\parallel} \mathbf{Y}_{xy}^{\parallel} \mathbf{v}_{xy}, \quad (\text{D.16})$$

where $\mathbf{v}_{xy} = \mathcal{B}_{xy} \left[\frac{s}{\rho^- h^-} (-\ell_0 p_n^- + \mathcal{L}_n^{(1)} \mathbf{P}^-) \mathbf{c}_{zx}^{[xy]} + \frac{1}{h^+} (\ell_0 v_z \mathbf{c}_{zz}^{[xy]} + \mathbb{P} \mathcal{C}_{zz}^+ \mathcal{L}_0^{(3)} \mathbf{V}^+) \right]$.

The last difficulty is to eliminate the acoustic pressure p_n^- from Eqs. (D.11), (D.13) and (D.16). After some algebra, we obtain the following equation:

$$\left\{ 1 - \frac{s^2 h^+}{\rho^- h^-} \underbrace{\mathbf{c}_{zx}^{[z]} \cdot \left[\mathbf{X}_{xy}^{\parallel} \mathbf{Y}_{xy}^{\parallel} (\mathcal{C}_{zz}^{[xy]})^{-1} \mathbf{c}_{zx}^{[xy]} \right]}_{c_{13} \text{ for orthorhombic crystals}} \right\} p_n^- = q(\phi_n^-, \Phi^-, \mathbf{P}^-, u_z, \mathbf{U}^+, \mathbf{r}_{xy}^\perp, \mathbf{V}^+), \quad (\text{D.17})$$

where $\mathbf{c}_{zx}^{[z]}$ is the 2D vector of components of the stiffnesses c_{13} and c_{36} . By construction, the function q does not depend on the acoustic pressure p_n^- . This function is very complicated. This is why the right-hand side of Eq. (D.17) is not detailed here. Note that a nonphysical singularity is unexpectedly introduced and can be treated by changing the discretization steps h^- and h^+ .

D.4.3 Homogeneous elastic solid/homogeneous elastic solid [Eq. (13), Table 2]

For nondegenerate cases, *i.e.*, $s \neq 1/c_i^-$ and $s \neq 1/c_i^+$ for $i = 1, 2, 3$, the continuity of displacement gives $\mathbf{u}_n^- = \mathbf{u}_0^+$, which implies $\mathbf{v}_n^- = \mathbf{v}_0^+$. Using the same notations as those for the *fixed-frequency problem*, see Eq. (C.20) by setting $\nu = 0$, the following set of equations is built:

$$\begin{cases} \mathbf{u}_n^- = -s \mathbf{X}^\perp \boldsymbol{\Lambda} \mathbf{r}^\perp + (\mathcal{A}^+ \mathcal{L}_0^{(3)} \mathbf{U}^+ - \mathcal{A}^- \mathcal{L}_n^{(3)} \mathbf{U}^-) \\ \mathbf{v}_n^- = \mathbf{X}^\perp \mathbf{r}^\perp + \mathbf{X}^{\parallel} \mathbf{Y}^{\parallel} (\mathcal{A}^+ \mathcal{L}_0^{(3)} \mathbf{V}^+ - \mathcal{A}^- \mathcal{L}_n^{(3)} \mathbf{V}^-) \\ i\omega \mathbf{r}^\perp = \frac{-1}{s} \boldsymbol{\Lambda}^{-1} \left[\mathbf{r}^\perp - \mathbf{Y}^\perp (\mathcal{A}^+ \mathcal{L}_0^{(3)} \mathbf{V}^+ - \mathcal{A}^- \mathcal{L}_n^{(3)} \mathbf{V}^-) \right] \end{cases} \quad (\text{D.18})$$

to bring to light the [interfacial state vector](#) $\mathbf{s}_I = \mathbf{r}^\perp$.

This set of equations gives all necessary expressions to obtain the form (13). As previously, if $\mathcal{C}_{zx}^- = \mathcal{C}_{zx}^+$, there is no interfacial state vector, *i.e.*, its rank r is zero. Therefore, analogous to the other problems given by Eqs. (B.17) and (C.21), Eq. (D.18) simply becomes: $\mathbf{u}_n^- = \mathcal{A}^+ \mathcal{L}_0^{(3)} \mathbf{U}^+ - \mathcal{A}^- \mathcal{L}_n^{(3)} \mathbf{U}^-$ and $\mathbf{v}_n^- = \mathcal{A}^+ \mathcal{L}_0^{(3)} \mathbf{V}^+ - \mathcal{A}^- \mathcal{L}_n^{(3)} \mathbf{V}^-$.